

**EVALUATION OF CYTOPROTECTIVE EFFECT OF
XANTHONES ISOLATED FROM *Calophyllum* spp. AND *Garcinia
parvifolia* AGAINST GLUTAMATE-INDUCED TOXICITY IN
BV2 MICROGLIA CELLS**

By

PNG WEN YANG

A Project report submitted to Department of Biomedical Science

Faculty of Science

Universiti Tunku Abdul Rahman

in partial fulfilment of the requirements for the degree of

Bachelor of Science (Hons) Biomedical Science

April 2018

ABSTRACT

EVALUATION OF CYTOPROTECTIVE EFFECT OF XANTHONES ISOLATED FROM *Calophyllum* spp. AND *Garcinia* *parvifolia* AGAINST GLUTAMATE-INDUCED TOXICITY IN BV2 MICROGLIA CELLS

Png Wen Yang

Excess extracellular glutamate can lead to glutamate-induced toxicity and eventually causes neurodegenerative diseases and stroke in both *in vitro* and *in vivo* settings. Xanthones with hydroxyl and prenyl groups have been shown to be neuroprotective against toxic insults. Therefore, the cytotective effect of euxanthone (EX) and ananixanthone (AX) isolated from *Calophyllum* spp. and rubraxanthone (RX) and 1,3,7 trihydroxy-2,4-bis (3-methylbut-2-enyl) (TX) isolated from *Garcinia parvifolia* against glutamate-induced toxicity was investigated in mouse microglia BV2 cells. The maximum non-toxic dose (MNTD) of four xanthones was determined prior to determining its cytoprotective effect. MTT assay was used to access the cell viability, and intracellular ROS generation was determined by DCFH-DA assay. Apoptosis was determined by observing nuclei morphological changes after staining with DAPI, followed by nuclei morphometric measurements by Image J software to obtain nuclear area factor. The MNTD of EX, AX, RX, and TX were 15.85 μ M,

10.23 μM , 0.89 μM , and 3.98 μM , respectively. Glutamate treatment alone in BV2 cells induced decrease in cell viability, with the high increment in intracellular ROS production, while the co-treatment of all four xanthenes with glutamate significantly increased cell viabilities by 14-22%, but with insignificant reduction in intracellular ROS production. In addition, the cell and apoptotic morphology analysis indicated mild membrane blebbing, less chromatin condensation, and higher nuclear area factor in BV2 cells co-treated with xanthenes and glutamate, suggesting that these xanthenes may inhibit glutamate-induced apoptosis in BV2 cells. In conclusion, the MNTDs of isolated xanthenes confer cytoprotective effect against glutamate-induced toxicity in BV2 cells by increasing in cell viability and inhibiting apoptosis, but less intracellular ROS attenuation. Therefore, detailed molecular mechanisms involved in the cytoprotective effect of xanthenes warrants further investigation.

ACKNOWLEDGEMENTS

First and foremost, I would like to express my sincere appreciation to my supervisor, Dr. Say Yee How for his motivation, aspiring guidance, and practical advices throughout the project. His productive recommendations guided me all the time during the research as well as in the thesis writing. I am also sincerely grateful to senior master student, Ms. Nor Anis Adila for the patience and guidance given throughout the research work. Also, I would like to thank Dr. Lim Chan Kiang for providing the xanthones chemicals and Dr. Sharmili Vidayadaran for providing the BV2 microglia cell lines in this project.

Furthermore, I would like to express my gratitude to laboratory officers, Mr Tie Shin Wei, Mr Gee Siew Meng, and Mr. Saravanan a/l Sivasangaran for their kind assistance and suggestions. In addition, I would also like to thank my fellow bench mates and course mates, who encouraged and supported me throughout the project.

DECLARATION

I hereby declare that the dissertation is based on my original work except for quotations and citations which have been duly acknowledged. I also declare that it has not been previously or concurrently submitted for any other degree at UTAR or other institutions.

PNG WEN YANG

APPROVAL SHEET

This dissertation entitled “**EVALUATION OF CYTOTECTIVE EFFECT OF XANTHONES ISOLATED FROM *Calophyllum* spp. AND *Garcinia parvifolia* AGAINST GLUTAMATE-INDUCED TOXICITY IN BV2 MICROGLIA CELLS**” was prepared by PNG WEN YANG and submitted as partial fulfillment of the requirements for the degree of Bachelor of Science (Hons) Biomedical Science at Universiti Tunku Abdul Rahman.

Approved by:

(Assoc. Prof Dr. Say Yee How)

Date:.....

Supervisor

Department of Biomedical Science

Faculty of Science

Universiti Tunku Abdul Rahman

FACULTY OF SCIENCE
UNIVERSITI TUNKU ABDUL RAHMAN

Date: _____

PERMISSION SHEET

It is hereby certified that **PNG WEN YANG** (ID No: **14ADB04247**) has completed this final year project entitled **“EVALUATION OF CYTOPROTECTIVE EFFECT OF XANTHONES ISOLATED FROM *Calophyllum* spp. AND *Garcinia parvifolia* AGAINST GLUTAMATE-INDUCED TOXICITY IN BV2 MICROGLIA CELLS”** under the supervision of Dr. Say Yee How from the Department of Biomedical Science, Faculty of Science.

I understand that University will upload softcopy of my final year project in pdf format into UTAR Institutional Repository, which may be made accessible to UTAR community and public.

Yours truly,

(PNG WEN YANG)

TABLE OF CONTENTS

	Page
ABSTRACT	ii
ACKNOWLEDGEMENTS	iv
DECLARATION	v
APPROVAL SHEET	vi
PERMISSION SHEET	vii
TABLE OF CONTENTS	viii
LIST OF TABLES	xii
LIST OF FIGURES	xiii
LIST OF ABBREVIATIONS	xv
 CHAPTER	
1	INTRODUCTION 1
2	LITERATURE REVIEW 5
2.1	Neuroprotection of Natural Compounds 5
2.1.1	Protective Effects of <i>Garcinia</i> spp. 5
2.1.2	Protective Effects of <i>Calophyllum</i> spp 7
2.2	Xanthone 8
2.2.1	Rubraxanthone Biological Activities 9
2.2.2	Euxanthone Biological Activities 9
2.2.3	Ananixanthone Biological Activities 10
2.2.4	Xanthones Act as Non-Enzymatic Antioxidant 10
2.3	Glutamate-induced Oxidative Stress 12
2.3.1	Glutamate Overview 12
2.3.2	Role of Glutamate Receptor in Microglial Death 13
2.3.3	Role of Glutamate Transporter and ROS Generations 16

2.4	Redox Biology System in Glutamate-Induced Toxicity	18
2.4.1	ROS and Antioxidant	18
2.4.2	Microglial Glutathione system	20
3	METHODS AND MATERIALS	22
3.1	Materials and Equipment	22
3.2	Reagents and Solutions Used	23
3.3	Preparation of Xanthenes Stock Solutions	25
3.4	BV2 Microglia Cells	25
3.5	Cell Culture	25
3.5.1	Culturing Medium Preparation	25
3.5.2	Thawing Cells	26
3.5.3	Subculturing Cells	27
3.5.4	Cryopreservation of Cell Line	28
3.5.5	Cell counting and Viability test	28
3.6	Bioassay	29
3.6.1	Maximum Non Toxic Dose (MNTD) Determination by MTT assay	29
3.6.2	Cell Viability Determination by MTT Assay	29
3.6.3	Intracellular Free Radical Production by DCFH-DA Assay	31
3.6.4	DAPI Nuclear Staining and Morphology Analysis	32
3.6.5	Image J Nuclear Morphology Analysis	32
3.7	Statistical Analysis	33
4	RESULTS	34
4.1	Maximum Non Toxic Dose (MNTD)	34

4.2	Neuroprotection of Xanthenes in Glutamate-Induced Cell Death	37
4.3	DCFDA ROS Generation Test	38
4.4	Cells Death Morphology Analyses	40
4.4.1	Inverted and Fluorescence Microscope Analysis	40
4.4.2	Quantification of Morphological Changes in Nuclei	43
5	DISCUSSION	45
5.1	Cytotoxic Profile for EX, AX, RX, and TX	45
5.2	Validity of Glutamate and Vitamin E as Control Group	47
5.3	EX, AX, RX, and TX Improved Cell Viability Against Glutamate Induced Toxicity	49
5.4	EX, AX, RX, and TX Did Not Attenuate ROS in Glutamate-Challenge BV2 cells	50
5.5	EX, AX, RX, and TX Prevent Glutamate-induced Apoptotic Changes in BV2 cells	53
5.6	EX, AX, RX, and TX Rescued BV2 Cells Nuclei Apoptotic Progression	54
5.7	Limitations of Study	56
5.7.1	<i>In vitro</i> Studies Not Necessarily Reflective of <i>in vivo</i> Clinical Studies	56
5.7.2	Microglia Culture Less Representative the Neuron-glia Interaction	57
5.7.3	Inconsistency in Experiment	57
5.8	Further Studies	58
6	CONCLUSION	60
	REFERENCES	62

LIST OF TABLES

Table		Page
2.1	Subtype of metabotropic and ionotropic receptors	13
3.1	Materials and equipment with brands names, and supplier countries	22
3.2	Reagent and solutions with brands and supplier countries.	23
3.3	Chemical structure, mass and molecular weight of the xanthone	24
4.1	MNTDs of the EX, RX, AX, and TX	37

LIST OF FIGURES

Figures		Page
2.1	Stem, leaves, and fruits of <i>Garcinia parvifolia</i>	6
2.2	Stem, leaves, and flowers of <i>Calophyllum antillanum</i>	7
2.3	Chemical structure of xanthone	8
2.4	Glutamate amino acid 2D structure	12
2.5	Interaction of Group II and Group III mGluR receptor with glutamate	15
2.6	Ions and glutamate movement across excitatory amino acid transporter (EAAT) and x_c^- glutamate/cysteine antiporter system	16
2.7	EAAT and x_c^- glutamate/cysteine antiporter system in the regulation of extracellular glutamate and ROS	18
2.8	Interaction of Superoxide and nitric oxide to form peroxynitrite	19
2.9	Structure of Glutathione	20
2.10	Interconversion of Redox State in Glutathione by Glutathione peroxidase and Glutathione Reductase	21
3.1	Layout of the positive control (Vitamin E + Glutamate) and negative control (Glutamate only) with co-treatment of xanthenes and glutamate.	30

4.1	Dose-dependent BV2 cell cytotoxicity against log ₁₀ concentration of (A) 1,3,7 trihydroxy-2,4- bis (3-methylbut-2-enyl) xanthone (TX), (B) Euxanthone, (C) Rubraxanthone (RX), (D) Ananixanthone (AX).	36
4.2	Effect of xanthoness treatment against glutamate-induced cell death on cell viability of BV2 cells.	38
4.3	Fluorescence reading of DCFH-DA for 10, 20, 30 and 60 mins.	39
4.4	Nuclei morphological observation of BV2 cells stained with DAPI staining (blue) by fluorescence microscope for controls and xanthoness treatments (magnification 10X).	42
4.5	Nuclear area and circularity relative to control cells was obtained from a population of at least 20 cells.	43
4.6	Nuclear area factor was calculated form the product of circularity and nuclear area	44

LIST OF ABBREVIATIONS

A β	Amyloid protein
AD	Alzheimer's disease
AMPA	α -amino-3-hydroxy-5-methyl-4-isoxazolepropionic acid receptor
AX	Ananixanthone
Bcl	B-cell lymphoma 2
Bax	Bcl-2 associated X
CNS	Central nervous system
DAPI	4',6-diamidino-2-phenylindole
DCFH-DA	Dichlorodihydrofluorescein diacetate
DF	Dilution factor
DMEM	Dulbecco's Modified Eagle's Medium
DMSO	Dimethyl sulfoxide
EAAT	Excitatory amino acid transporter
EDTA	Ethylenediaminetetraacetic acid
ERK	Extracellular Signal-regulated Kinase
EX	Euxanthone

Fas	First apoptosis signal receptor
FasL	First apoptosis signal receptor ligand
FGF	Fibroblast growth factor
FBS	Fetal bovine serum
GLCZD	Gua Lou Gui Zhi
Glu	Glutamate
GluR	Glutamate receptor
GO	Glutathione oxidase
GSH	Glutathione
GSHPx	Glutathione peroxide
GSSG	Glutathione disulphide
IGluRs	Ionotropic Glutamate Receptors
GR	Glutathione reductase
IP ₃	Inositol-1,4,5-triphosphate
JNK	c-Jun N-terminal kinases
KA	Kainate
LOO [•]	Lipid peroxy radical

MAP-2	Mircotubule associated protein 2
mGluR	Metabotropic glutamate receptor
MMP	Metalloproteinases
MNTD	Maximum non-toxic dose
MTT	3-(4,5-dimethylthiazol-2-yl)-2,5-diphenyltetrazolium Bromide
NAF	Nuclear area factor
NADH	Nicotinamide adenine
NMDA	<i>N</i> -methyl-D-aspartate
NOX	NADPH oxidase
NR	NMDA receptor subunits
OHDA	6-hydroxydopamine
PAF	Platelet activating factor
PBS	Phosphate buffered saline
PKC	Protein kinase C
ROS	Reactive oxygen species
RX	Rubraxanthone

SEM	Standard error of the mean
SET	Single electron transfer
SOD	Superoxide dismutase
TX	1,3,7 trihydroxy-2,4- bis (3-methylbut-2-enyl) xanthone
Wnt	Wingless-type MMTV (mouse mammary tumor virus) integration site
xCT	Sodium-independent cystine-glutamate antiporter

CHAPTER 1

INTRODUCTION

Natural phytochemical products have been discovered to treat different kinds of diseases, and these phytochemicals include the host product of plant species and its compound derivatives (Kumar and Khanum, 2012). Phytochemicals are able to maintain the chemical balance of the brain by influencing the inhibitory neurotransmitter interaction with its receptors. Several plants or medicinal herbs contain active phytochemical compounds like phenol, alkaloid, fatty acids, terpenes, saponins, and flavonoids. These compounds showed resistance against different stress signals by promoting specific transcription factors and signal transduction pathways (Rocha, et al., 2011). On the other hand, phytochemicals also direct uptake of free radicals, and promote radical scavenging activity involved in chelation of divalent cation in Fenton reactions. Furthermore, phytochemicals also regulate antioxidant enzyme and enhance free radicals scavenging activity in central nervous system (Upadhyay and Dixit, 2015). For instance, a polyphenolic compound known as flavonoid is found in vegetables and fruits. With its high content of antioxidant capacity, it can overcome oxidative damage (Pérez-Hernández, et al., 2016).

Over these years, xanthone compounds were extracted from various plant species like *Cudrania tricuspidata* (Kwon, et al., 2014), *Swertia punicea* (Du, et al., 2010), *Garcinia mangostana* (Zhang, et al., 2010), and *Hypericum*

monogynum (Xu, et al., 2016) have shown its neuroprotective properties towards different stressors in *in vitro* neuronal cell studies. Although there were abundant studies focused on the neuroprotective effects of xanthenes, but there are very little scientific investigations on the protective effect in glial cells. Similar to neurons, glutamate can induce toxicity effect in glial cells such as microglial, oligodendrocyte and astrocytes. These glial cells express different glutamate receptors and transporters which mediate the damaging effects of glutamate (Matute, Domercq, and Sanchez-Gomez, 2006). Neuroglia cells are vital in maintaining the normal function of neurons. It exerts its function via a rapid regulatory mechanism to rescue the cell from stress or being injured. Among all the glial cells, microglia cells show its function in maintaining the CNS homeostasis and confer protection against pathological conditions in CNS (Chen and Trapp, 2016). On the other hand, microglia cells also modulate the neuronal synapse to protect the neurons against the traumatic injuries, as well as promoting neurogenesis. Furthermore, microglia cells also attenuate neuroinflammation in diseases like Alzheimer's disease, stroke, and autism (Howe and Barres, 2012). Therefore, it is vital to prevent microglial cell death, because any damage or impairment on microglia cells could result in a critical effect to the brain function and eventually contributes to the cognitive dysfunction (Kumar and Khanum, 2012).

Glutamate-induced toxicity is associated with the increase of glutamate release in CNS. The increments are mostly due to trauma, hypoxia-ischemia conditions or metabolic associated failures. As glutamate accumulate excessively in CNS, it causes excitotoxicity and several neurological disorders due to the impairment

of the transport system and uptake mechanism (Mallick, 2007). In post-ischemic stroke or Alzheimer's disease, there are evidence which showed de novo expression of glutamate receptor (GluR) in microglial cells (Matute, et al., 2006). The increase in GluR would promote the sustained activation of receptor and result in microglia cell death, for instance, as glutamate binds strongly to Group II mGluR, it results in depolarization and apoptosis (Fry, 2009).

In addition, high glutamate concentration also inhibits glutathione synthesis by reducing the cysteine uptake which indirectly causes the impairment in cellular antioxidant system and increase in reactive oxygen species (Matute, Domercq and Sanchez-Gomez, 2006). To prevent microglia cell death, cytoprotective effect of four recently isolated natural xanthone compounds were tested on mouse microglia BV2 cells. Among the four xanthenes tested, euxanthone (EX) and ananixanthone (AX) were extracted from *Calophyllum spp.*, while the 1,3,7 trihydroxy-2,4- bis (3-methylbut-2-enyl) xanthone (TX), and rubraxanthone (RX) were isolated from *Garcinia parvifolia*.

The purpose of this research was to investigate the cytoprotective properties and cytoprotective mechanism of the natural xanthenes compounds against the glutamate induced toxicity. To fulfil this purpose, the objectives were as follows:

1. To determine the Maximum non-toxic dose (MNTD) of EX, AX, RX, and TX in BV2 microglial cell line.
2. To investigate the ability of EX, RX, AX, and TX to reduce the glutamate-induced toxicity by accessing the cell viability at their respective MNTD.

3. To determine the antioxidant activity of EX, RX, AX, and TX by measuring intracellular ROS production in glutamate-induced BV2 cell line.
4. To study the mode and progression of cell death by observation on nuclei morphology counterstained with DAPI, and quantification of the nuclear morphometric analysis by nuclear area factor.

CHAPTER 2

LITERATURE REVIEW

2.1 Neuroprotection of Natural Compounds

Natural compounds have a wide range of pharmacological and therapeutic effects. These complex chemical compounds exhibit protective effect against oxidative stress by targeting various signalling pathways and regulate the gene expression of enzymes like regulatory protein and kinases (Harvey and Cree, 2010). Furthermore, natural compounds also regulate the cascade of molecular and cellular activities like mitochondrial dysfunction, excitotoxicity, inflammation, oxidative stress, protein misfolding and apoptosis (Bagli, et al., 2016). In previous study, xanthones isolated from *Garcinia parvifolia* (Tang, et al., 2013) and *Calophyllum* spp, (Taher, et al., 2010) have shown its protective effects against different stressors.

2.1.1 Protective Effects of *Garcinia* spp.

Garcinia are a genus originated from tropical family Guttiferae which are rich in bioactive natural compounds such as xanthones and bioflavonoids (Xu, et al., 2001). The stems, leaves, and fruits of *Garcinia* spp shown in Figure 2.1 have shown wide therapeutic effects in different diseases. Previously, methanolic extract from *Garcinia indica* fruits had shown its protective effects in the rat's dopaminergic neurons against 6-OHDA-induced toxicity (Antala, et al., 2012).

In addition, one of the *Garcinia indica* extracts known as garcinol also demonstrated anti- tumorigenic effect and show potential chemopreventive effect (Tang, et al., 2013).



Figure 2.1: Stem, leaves, and fruits of *Garcinia parvifolia* (Adapted from National Park Board, 2013).

Several compounds extracted form *Garcinia gracillis* also showed protective effect in preventing DNA damage, and exerting neuroprotective effects. One of the compound extracted from *Garcinia gracillis* known as apigenin-8-*C*- α -L-rhamnopyranosyl-(1 \rightarrow 2)- β -D-glucopyranoside prevented DNA damage induced by photochemical reaction, and prevented oxidative damage in P19-derived neuron (Supasuteekul, et al., 2016).

The protective effect against H₂O₂-induced apoptosis is also evident in the *Garcinia xanthochymus* extract. After treatment by the compound, the cell viability increased significantly, with decrease in the lipid peroxidation and increase in activities of antioxidant enzyme such as catalase, superoxide dismutase, and heme oxygenase-1 (Xu, et al., 2017). In addition, reactive oxygen (ROS) level and matrix metalloproteinases (MMP) also decreased after treatment. Furthermore, *Garcinia xanthochymus* extract treatment also

indicated a decrease in cytochrome *c* and Bax expression, which contribute the decrease in Bax/Bcl-2 ratio (Xu, et al., 2017).

2.1.2 Protective Effects of *Calophyllum* spp.

Calophyllum are also known as Clusiaceae or Guttiferae. Until today, there are 180-200 different species found in *Calophyllum*, which allows a wide isolation and analysis of different natural compounds like xanthone, ketones, coumatins, bioflavonoids, and chalcones. These natural active compound are extracted from the stem, leaves, and flowers of *Calophyllum* spp as shown in Figure 2.2. Previously, *Calophyllum* spp. were also used as traditional medicine which exhibit therapeutics effects, such as anti-microbial, anti-cancer, anti HIV, antifungal and antioxidant (Shagufta and Ahmad, 2016). The antioxidant activities used for scavenging the free radicals and lipid peroxidation inhibition were evident in the leaves of *Callophyllum rubugunosum* (Taher, et al., 2010).



Figure 2.2: Stem, leaves, and flowers of *Calophyllum antillanum* (Adapted from National Museum of Natural History, 2018).

On the other hand, antioxidant and anti-cholinesterase activity were also found in the phenolic extract isolated from *Calophyllum symingtonianum* and *Calophyllum depressinervosum* (Taher, et al., 2010). The antioxidant activities were able to reduce the incident of oxidative stress caused by ROS, while the

anti-cholinesterase activities prevented the decline of acetylcholine level in the Alzheimer's patients (Ee, *et al.*, 2015)

2.2 Xanthenes

Xanthone is a polyphenolic compound with three aromatic rings as shown in Figure 2.3. It is a common secondary metabolite which are found in higher plant family, lichen and fungi. These compounds are mainly extracted from plants such as Moraceae, Guttiferae, Gentianaceae, Clusiaceae, and Polygalaceae. Although, xanthenes are polyhydroxylated compounds in majority, but they also exists as glycosides, and polymethyl ethers compounds (Negi, *et al.*, 2013). Furthermore, xanthenes also exert wide range of pharmacological response such as anti-microbial, antithrombotic, anti-inflammatory and protective effects (Yoswathana and Estiaghi, 2015). In this study, euxanthone (EX) and ananixanthone (AX) were extracted from *Calophyllum spp.*, while the 1,3,7 trihydroxy-2,4- bis (3-methylbut-2-enyl) xanthone (TX), and rubraxanthone (RX) were isolated from *Garcinia parvifolia*. Although, research on biological properties had been carried out in EX, AX, RX, but there have been less investigations on TX, as it is a newly discovered compound.

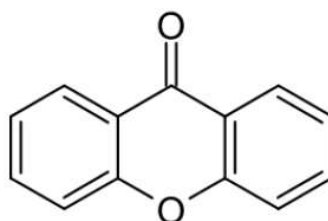


Figure 2.3: Chemical structure of xanthone (Adapted from Machmudah, *et al.*, 2015).

2.2.1 Rubraxanthone Biological Activities

Rubraxanthone (RX) extracted from different sources showed anti-platelet activation, antimicrobial, anticancer and anti-inflammatory properties. For instance, RX isolated from *Garcinia parvifolia* inhibit the platelet activating factor (PAF) by reducing the specific binding of the PAF receptor to PAF (Jantan, et al., 2002). With this inhibition activity, RX maybe used to treat many diseases, such allergy, inflammation, asthma, and thrombosis (Jantan et al., 2002). On the other hand, RX isolated similarly form *Garcinia parvifolia* showed its strong antimicrobial activities against penicillin resistance *Staphylococcus aureus*, while there is a moderate effect against *Microsporium gypseum* and *Trcihophyton mentahrophytes* (Pattalung, et al., 1987). Furthermore, RX extracted from the root bank of *Garcinia magostana* also showed its potential in exerting anti-cancer effect against the CEM-SS lymphoblastic leukaemia cell line (Ee, et al., 2006). Also, RX derived from *Garcinia cowa* also showed its anti-inflammatory effect by inhibiting 23.86% of NO released (Wahyuni, et al., 2016).

2.2.2 Euxanthone Biological Activities

Euxanthone (EX) functions mainly in neuronal differentiation, antifungal, and vasodilator effect. Previously, neuronal differentiation of neuroblastoma BU-1 cell line with the increase in expression of specific neurite marker MAP-2 was stimulated by EX extracted from the *Polygala caudate* (Nai-Ki, et al., 1999). While another research indicated mRNA expression of the neural growth and differentiation factor such as protein kinase C (PKC) also increased after EX

treatment (Naidu, et al., 2007). In addition, EX isolated from *Garicinia mangostana* also showed antifungal activity against the pathogenic fungi such as *Fusarium oxysporum vasinfectum*, *Alternaria tenuis*, and *Dreschlera oryzae* (Gopalakrishnan, Banumathi and Suresh, 1997). Besides, EX also induced vasodilation which independent from the effect from endothelial growth factor such as nitric oxide. The detailed EX vasodilator effect involved activation of protein kinase C which resulted in the inhibition of calcium dependent mechanism (Câmara, et al., 2010).

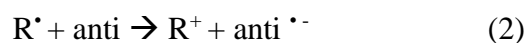
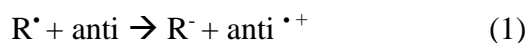
2.2.3 Ananixanthone Biological Activities

Ananixanthone (AX) exerted anticancer, antibacterial, and antioxidant properties. Previously, the cytotoxic properties towards cancer cell line such as LST174T colorectal adenocarcinoma cell line, SNU-1 gastric carcinoma cell line and K562 chronic myelogenous leukaemia cell line were evident in ananixanthone extracted from *Calophyllum teysmannii* (Lee, et al., 2017). On the other hand, AX also exhibited antioxidant activities by scavenge the free radicals and inhibition toward the growth of *S. aureus*, *E. faecalis*, *B. cereus*, *P. aeruginosa*, *E. coli*, and *S. typhimurium* (Fouotsa, et al., 2015).

2.2.4 Xanthenes Act as Non-Enzymatic Antioxidant

The analysis of xanthone's antioxidant function is vital to study relationship between the antioxidant nutrient intake in a variety of epidemiological research. Antioxidant mechanism of xanthone utilizes the single electron transfer

mechanism (SET), which transfers electron to and from the free radicals (Martinez, et al., 2012).



Reaction 1 shows the ROS scavenger act as antioxidant, while reaction 2 shows an anti-reductant reaction. The dual mechanism in SET are dependent on the nature of free radical and the structural characteristics in antioxidants, while the effectiveness of antioxidants depends on ionization energy and electron affinity. The lower the ionization energy, the higher efficiency an antioxidant act as an electron donor. In contrast the higher the electron affinity, the better an antioxidant act as electron acceptor (Martinez, et al., 2012).

The study of xanthone effect on the free radicals such as OH^{\bullet} and $\text{O}_2^{\bullet-}$, indicated the ability of xanthone to scavenge and deactivate the free radicals by either donate or accept electron. Besides, it is able to trap and delay or inhibit the oxidative chains action of free radicals. The antioxidant effect is important in preventing the disease caused by oxidative stress such as brain dysfunction, ischemic stroke and AD (Martinez, et al., 2012). For instance, Gua Lou Gui Zhi, a Chinese medicine consist of galloyl glucose, phenolic acid, flavonoid, gingerols, and glucosides (Xu, et al., 2015) exhibited neuroprotective effect in cerebral ischemia and reperfusion injury by the regulation of antioxidants pathways (Zhang, et al., 2015).

2.3 Glutamate-Induced Oxidative Stress

2.3.1 Glutamate Overview

Glutamate is amino acid which functions as a neurotransmitter in the brain and stimulate neuroplasticity such as learning, emotion, memory, motor and sensory function (Mattson and Magnus, 2006). This amino acid is made up of a α carbon, which is located at the centre, forming a bond with amino group (NH_3) and carboxyl group (COOH), with a side chain of $\text{CH}_2\text{CH}_2\text{COO}^-$ bonded to α carbon. The glutamate in cerebral cortex is derived from α ketoglutarate which is a product from Krebs cycle or citric acid cycle (Mark, et al., 2001).

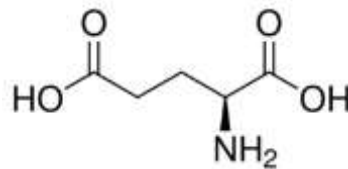


Figure 2.4: Glutamate amino acid 2D structure (Adapted form Sigma-Aldrich, 2017).

Glutamate is first synthesized in endoplasmic reticulum like most of the neurosecretory substances, and transported to golgi apparatus for further modification. The two major receptors involved are metabotropic and ionotropic receptors (Harvey and Shahid, 2012). The differences of these receptor are ionotropic receptors coupled to membrane ion channel directly while metabotropic receptors couple to the intermediate compounds or secondary messenger like G protein, cyclic nucleotide and inositol-1,4,5-triphosphate (IP_3). Three subtype of ionotropic receptors, are NMDA (*N*-methyl-D-aspartate), kainite and AMPA (a-amino-3-hydroxy-5-methyl-4-isoxazolepropionate),

while metabotropic receptors divided into group I, group I and group II as shown in Table 2.1 (Beneyto, et al., 2007).

Table 2.1: Subtype of metabotropic and ionotropic receptors (Table adapted from Fry, 2009)

Ionotropic glutamate receptors			Metabotropic glutamate receptors		
NMDA	AMPA	kainate	Group I	Group II	Group III
NR1	GluR 1	GluR 5	mGluR1	mGluR2	mGluR4
NR2A	GluR 2	GluR 6	mGluR5	mGluR3	mGluR6
NR2c	GluR 3	GluR 7			mGluR7
NR2D	GluR 4	KA 1			mGluR8
NR3A		KA 2			
NR3B					

NMDA, N-methyl-D-aspartate; NR, NMDA receptor subunits; AMPA, α -amino-3-hydroxy-5-methyl-4-isoxazolepropionic acid receptor; GluR, glutamate receptor; KA Kainate; mGluR, metabotropic glutamate receptor

2.3.2 Role of Glutamate Receptors in Microglial Death

Ionotropic Glutamate Receptors (iGluRs) are also known as cation-specific ion channel, which it is further classified into AMPA, kainite, and NMDA according to their binding properties. These receptors are not only present in postsynaptic neuronal cells for fast synaptic action potential transmission, but are also found in microglia cells. (Liu, et al., 2016). The function of iGluRs are induce electrophysiological responses, ATP release, TNF α release, and immediate early gene expression in *in vitro* microglia cells (Liu, et al., 2016). In previous studies, NMDA receptor showed increase in the release of TNF α ,

IL-1 and nitric oxide (Fry, 2009) and is evident in CNS injury (Kaur, et al., 2006). In ischemic conditions, NMDA receptor expression was found upregulated and caused the periventricular white matter damage in hypoxic postnatal rat model (Domercq, Villoldo and Matute, 2013).

On the other hand, metabotropic glutamate receptors (mGluRs) are composed of a seven transmembrane domain receptor that is coupled with a secondary messenger system and ion channels (Liu, et al., 2016). In the case of Alzheimer's disease, amyloid plaques enhance the release of microglial glutamate and bind to the group II mGluR in microglia cells to form a toxicity feedback loop. The binding causes group II mGluR to act as agonist which result in neurotoxic and apoptosis in microglia cells as shown in Figure 2.5. In contrast, group III mGluR receptor induced lesser activation with no toxicity effects (Taylor, Diemel and Pocock, 2003). Group III mGluR, such as mGlu4, mGlu5 and mGlu8 are found on microglia cells but they induce lesser binding affinity towards glutamate as compared to group II mGluR. As shown in a previous study, activation of group III mGluR reduced neuro-inflammation and microglial toxicity caused by LPS and β - amyloid (Liu, et al., 2016). Overall, the previous finding showed group II mGluR might induce toxicity, while the group III mGluR may exert protective effects. However, a recent controversial study suggested that ROS productions were associated with the activation of mGlu3 and group III mGluR, which induced activation of NADPH oxidase (NOX) enzyme (Haslund, et al., 2016). NOX enzyme is the main ROS generator which caused the CNS disease progression such as schizophrenia, and amyotrophic lateral sclerosis. Therefore, activation of mGlu3 and group III

receptor will cause downstream activation of NOX enzyme and production of ROS (Harrigan, et al., 2008). Furthermore, glutathione (GSH) depletion hypothesis indicated the activation of group III mGluR will decrease the expression of xCT, which cause decrease in cysteine uptake. Low intracellular cysteine level would result in inhibited GSH synthesis and impair the intracellular antioxidant protective system (Fry, 2009).

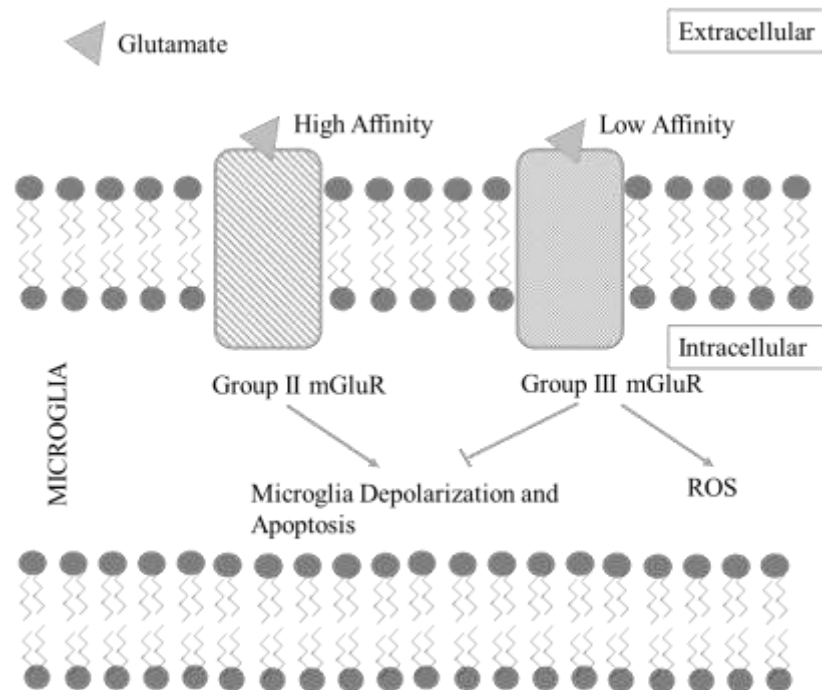


Figure 2.5: Interaction of Group II and Group III mGluR receptor with glutamate (Adapted from Liu, et al., 2016).

2.3.3 Role of Glutamate Transporter and ROS Generations

Glutamate transporters in microglia cells are divided into excitatory amino acid transporter (EAAT) and x_c^- glutamate/cysteine antiporter system as shown in Figure 2.6.

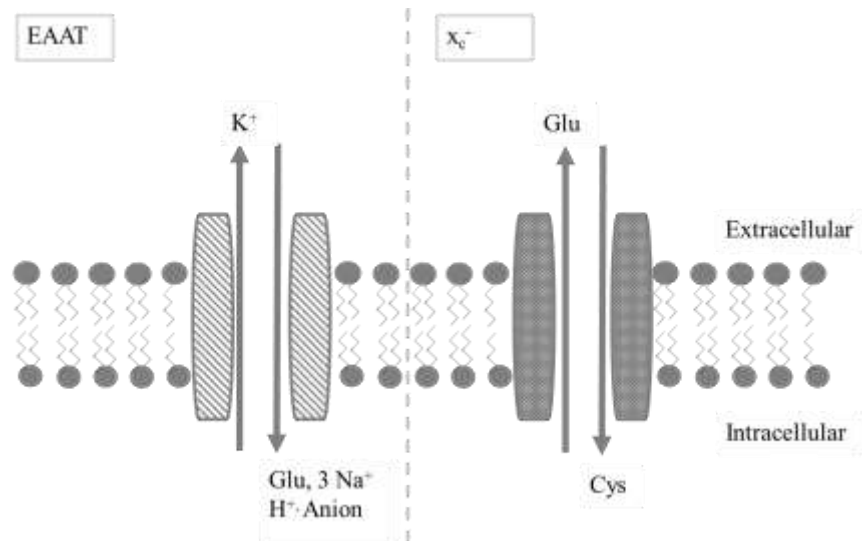


Figure 2.6: Ions and glutamate movement across excitatory amino acid transporter (EAAT) and x_c^- glutamate/cysteine antiporter system (Adapted from Fry, 2009).

EAAT high glutamate-uptake mechanism is dependent on the Na^+ gradient. While the level of Na^+ gradient is maintained by ATPase pump, enabling the glutamate uptake against its concentration. As one K^+ is transported out, three Na^+ are cotransported with one glutamate and one proton into the cells. Consequently, extracellular glutamate concentration can be regulated via EAAT to prevent any excessive glutamate toxicity effects (Fry, 2009).

The EAAT1, EAAT2, and EAAT3 activity might depend on the cellular redox environment. Previously, a study indicated that increase in ROS and thiol oxidising compounds reduced glutamate uptake into the cells as shown in Figure

2.7. The inhibited glutamate uptake maybe due to the formation of disulphide bond between the EAAT functional subunits, or the lipid peroxidation. However, the antioxidant compound can be used to antagonist the increased ROS environment and re-enable the glutamate uptake mechanism (Begni, et al., 2004).

Among all the cells in CNS, only microglia and astrocyte express the x_c^- system (Qin, 2006). The x_c^- glutamate/cysteine antiporter system or electroneutral antiporter, promotes the glutathione synthesis by importing the cystine into the cells in exchange of glutamate. However, in high extracellular glutamate conditions, the uptake of cysteine is inhibited and the x_c^- transporter may reverse its function to release the cysteine instead of uptake it. As the uptake of cysteine decreases, the precursor substances for glutathione enzyme synthesis also decrease. This would cause insufficient GSH enzyme production to reduce ROS intracellularly. Therefore, ROS level might increase with the increase of extracellular glutamate. In addition, at low cysteine concentration, this antiporter system also partially depends on Cl^- levels (Fry, 2009) .

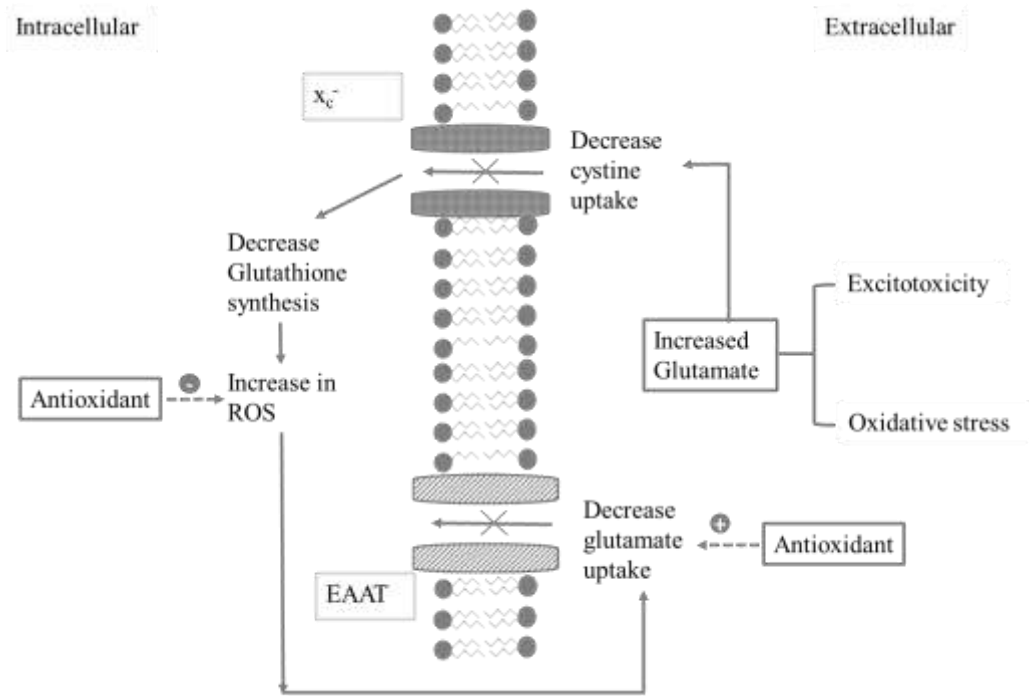


Figure 2.7: EAAT and x_c^- glutamate/cysteine antiporter system in the regulation of extracellular glutamate and ROS (Adapted from Fry, 2009).

2.4 Redox Biology System in Glutamate-Induced Toxicity

2.3.1 ROS and Antioxidant

Redox state in cells is critical in maintaining cell proliferation and viability. The shifting of redox balance state from antioxidant to oxidants is known as oxidative stress (Yang and Lee, 2015). Oxidative stress is often associated with certain diseases and conditions like in neurological disorders and ischemic stroke. Antioxidant enzymes are important redox biomarker and indicators for various diseases, as they function in the regulation of the functional protein's redox state (Yang and Lee, 2015). In high extracellular glutamate environment, ROS are released and causes damage to lipids, proteins and nucleic acids. Therefore, an intricate antioxidant network of superoxide dismutase (SOD), Glutathione (GSH), and catalase are present in the cell system to prevent the

adverse effect exerted by ROS (Birben, et al., 2012). Furthermore, there are also non-enzyme antioxidants with low molecular weight, such as β -carotene, ascorbic acids, and α -tocopherol function in reducing oxidative stress. Among all the antioxidants, GSH is more prominent to glutamate-induced toxicity study, as glutamate-glutathione (GSH) regulations mechanism are largely involved in the ROS regulation (Birben, et al., 2012).

Nitric oxide synthase also activated by glutamate, which it functions to form nitric oxide. As nitric oxide is produced, it may interact with superoxide to form toxic substances like peroxynitrite as shown in Figure 2.8 and result in neuronal death (Brown, 2007). Besides, nitric oxide can inhibit mitochondria respiration and damage DNA, which cause the increase in free radical production and leads to subsequent membrane depolarization. The neurotoxic event induced by nitric oxide is an important cascade in many cell death related to neurodegenerative disorder like Huntington's disease (Brown, 2010).

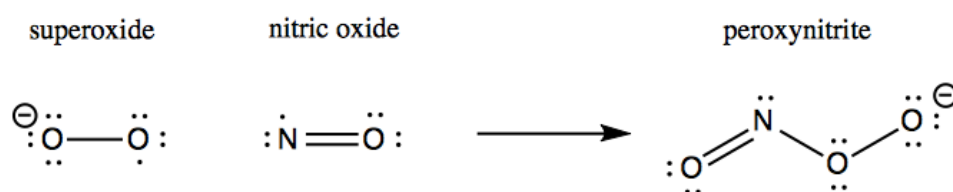


Figure 2.8: Interaction of Superoxide and nitric oxide to form peroxynitrite (Adapted from Minikel, 2015).

2.3.2 Microglial Glutathione system

Glutathione (GSH) or γ -L-glutamyl-L-cysteinylglycine is a thiol which consists of three peptides of L-cysteine, L-glutamate, and L- glycine.

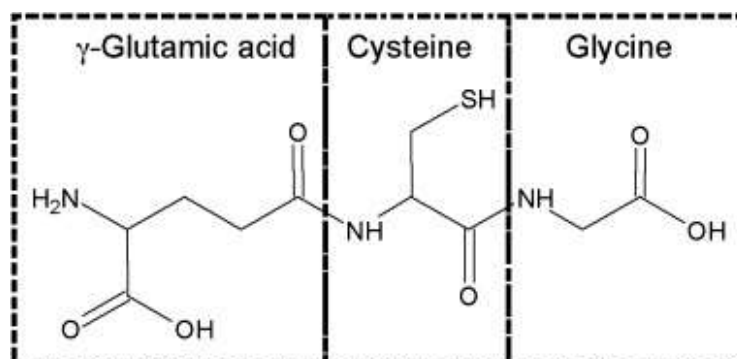


Figure 2.9: Structure of Glutathione (Adapted from Kawakami, Gledhill and Achterberg, 2006).

In microglial cell metabolism, ROS is produced resulted from the glutamate-induced oxidative stress as shown in Figure 2.5 and Figure 2.7. However, this oxidative effect is protected by the antioxidant GSH present in microglia cells. Among all the CNS cells, microglia cell is the best model to study the protection effect against glutamate oxidative stress, because it has the highest GSH level at 25 -40 nmol mg⁻¹ protein (Fry, 2009).

There are three enzymes that regulate the redox cycle of glutathione, such as glutathione reductase (GR), Glutathione oxidase (GO), and glutathione peroxidase (GSHPx). GO and GSHPx function to oxidize the GSH to GSSG glutathione disulphide. In contrast GR is responsible to restore the GSH level from GSSG via NADH-dependent process (Nimse and Pal, 2015). The redox regulation by these enzyme is shown in Figure 2.10.

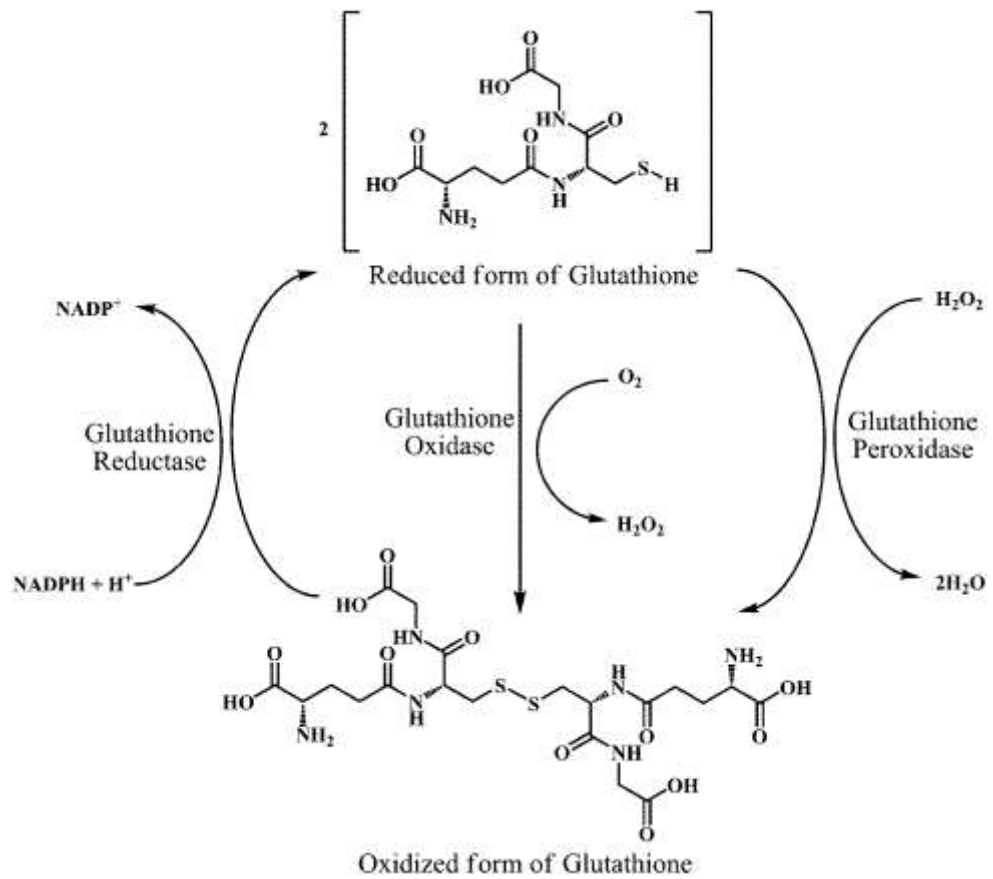


Figure 2.10: Interconversion of Redox State in Glutathione by Glutathione peroxidase and Glutathione Reductase (Adapted from Nimse and Pal, 2015).

CHAPTER 3

MATERIALS AND METHODS

3.1 Materials and Equipment

The material and equipment are listed in Table 3.1 with the company name and brands.

Table 3.1: Materials and equipment with brands names, and supplier countries

Material and Equipment	Brands and Supplier Countries
Cell culture 96-wells plate flat bottom	NEST, San Diego, Canada
10ml Serological Pipette	NEST, San Diego, Canada
Tissue culture 96-wells black plate	SPL, Geumgang-ro, Korea
T25 and T75 Cell culture flask	SPL, Geumgang-ro, Korea
S1 Pipet Fillers	Thermo Scientific, Massachusett, USA
Nikon Eclipse Ti-S Inverted microscope	Nikon instruments INC, Melvilli, New York, USA
Nikon Intensilight C-HGFI	Nikon instruments INC, New York, USA
QICAM Digital CCD camera	Qimaging, Burnaby, Canada
FLUOstar Omega filter-based multi-mode microplate reader	BMG Labtech, Ortenberg, Germany
Acrodisc membrane filters	Pall Cooperation, New York, USA
10 ml Sterile Syringe	Terumo, Laguna Philippines

3.2 Reagents and Solutions Used

The reagent and solutions used are listed in Table 3.2 with the company name and brands.

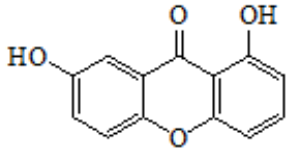
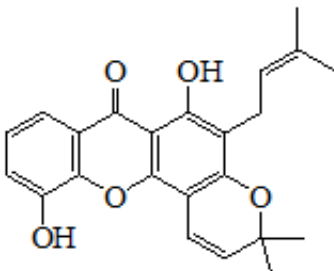
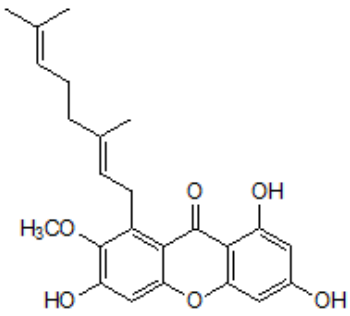
Table 3.2: Reagent and solutions with brands and supplier countries.

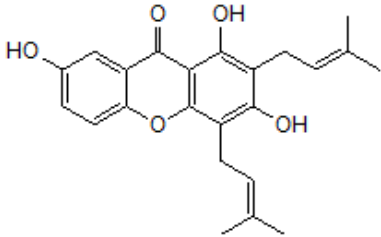
Reagents and Solutions	Brands and Company Names
Dimethyl Sulfoxide	Fisher Chemical, Leicestershire, United Kingdom
L- glutamic acid	Bio Basic, Amherst, New York, USA
Fetal Bovine Serum	TICO Europe, Amstelveen, Netherlands
2,7, dichlorofluorescin diacetate	Calbiochem, Darmstadt, Germany
Penicillin- Streptomycin Mixture solutions	Nacalai Tesque, Kyoto, Japan
Trypsin EDTA Solution A	Biological Industries, Cromwell, CT, USA
3-(4,5-dimethylthiazol-2-yl)-2,5-diphenyltetrazolium dye	Calbiochem, Darmstadt, Germany
Dulbecco's Modified Eagle's Medium (DMEM)	Corning, New York, USA
Triton X-100	Thermo Scientific, Massachusetts, USA
DAPI (4',6-diamidino-2-phenylindole)	Calbiochem, Darmstadt, Germany

3.3 Preparation of Xanthone Stock Solutions

Four xanthenes extract powder were obtained from Asst. Prof. Dr. Lim Chan Kiang at Department of Chemical Science, Faculty of Science, UTAR. Different xanthenes were weighted and dissolved in 1 ml of 100% DMSO solution (Fisher Chemical, Leicestershire, UK) to obtain a 10 mM concentration of stock solutions. The stock solutions were filtered with Acrodisc Syringe filters (Pall Cooperation, New York, USA) before storage under -20°C until further use.

Table 3.3 Chemical structure, mass and molecular weight of the xanthone

Xanthenes	Structure	MW (g/mol)
Euxanthone		228.203
Ananixanthone		378.424
Rubraxanthone		410.466

Xanthenes	Structure	MW (g/mol)
1,3,7-trihydroxy-2,4-bis(3-methylbut-2-enyl) xanthone		380.163

3.4 BV2 Microglia Cells

BV2 microglial cell were a gift from Dr. Sharmili Vidayadaran, Universiti Putra Malaysia. This is a retroviral immortalized adherent macrophage cell lines obtain from the brain tissue of *Mus musculus* mouse. Most frequent, this cell line is a substitute for the primary microglial cells, as BV2 immortalized cells have similar function as primary microglial cells, but with a lesser magnitude of response. Besides, these cell lines also useful in pharmacology studies, protective effects and many immunological discoveries.

3.5 Cell Culture

3.5.1 Culture Medium Preparation

Two empty schott bottles and 890 ml distilled water was autoclaved for sterilization purpose. About 3.7 g DMEM powder (Corning, New York, USA) was weighed and added into autoclave distilled water followed by 3.7 g sodium bicarbonate (NaHCO_3) and mixed well. The media pH was adjusted to the range of 6.9 to 7.1, and filtered equally into two schott bottle using 0.22 μM pore size

membrane filter with vacuum filter system. Then, 10 ml of penicillin-streptomycin mixture solutions (Nacalai Tesque, Kyoto, Japan) was added into DMEM and stored at 4°C. To confirm the sterility of the medium, 3 ml of the medium from each bottle was pipetted into tissue culture dishes and was parafilmmed before incubated in 37°C, 5% CO₂ humidified incubator. The culture dish was observed in aspect of the turbidity, and colour change due to pH change for 4 days on daily basis. to ensure the sterility of the culture. If the medium turns cloudy and yellowish it might indicate microbial contamination.

3.5.2 Thawing cells

Two flasks were prepared with complete culture medium. The vials were collected from the liquid nitrogen and quickly thawed in a preheat water bath at 37°C. The cell culture was resuspended quickly and divided equally 1 ml into each flask, and the flasks were store in 37°C 5% CO₂ humidified incubator. After 4-6 hrs, the media was changed to remove the DMSO, and the cells were observed under the microscope to ensure the cell viability. After cell observation, the flasks were stored back in 37°C 5% CO₂ humidified incubator.

3.5.3 Sub culturing Cells

DMEM media and FBS (TICO Europe, Amstelveen, Netherlands) were warmed at 37°C water bath first, then the cells were observed to ensure the confluency reached 70-90%. The medium was removed from the flasks and rinsed with 3ml of PBS once to remove the dead cells. After washing, the left over PBS was aspirated, and 1 ml trypsin EDTA solution (Biological Industries, Cromwell, CT, USA) was added, followed by incubation period of 10 min at 37°C 5% CO₂ humidified incubator for detachment of cells from the flasks. Trypsinised cells were observed under the microscope to ensure the cell detachment. Afterward, 2 ml of complete medium was added into the flasks to inactivate the trypsin action. Next, all the cells were pipette into 15 ml centrifuge and centrifuged at 800 g, at 25°C for 10 min. The supernatant was discarded and the pelleted cells was suspended with 1ml culture medium DMEM. About 150 µl of resuspended cell was transferred into T25 culture flask with pre-added 5 ml DMEM solutions. The flask was moved horizontally and vertically to ensure the even distribution of cells. At last, the subcultured cells were stored stored at 37°C 5% CO₂ humidified incubator.

3.5.4 Cryopreservation of Cell Line

To ensure healthy state of cells, the morphology of cells and the quality of medium was observed before the trypsinisation of cells. The similar procedure in section 3.5.3 was used to harvest the cells. Trypsinized cells were resuspended with 1ml of freezing medium (DMEM, pH 6.9 -7.1, 10% FBS, 1% Penicillin- Streptomycin and 5% DMSO) at cell density of 2.0×10^6 cell/ml in cryogenic vial, and store in freezer at -80°C .

3.5.5 Cell counting and Viability test

The trypsinised cells in section 3.5.3 were resuspended in growth medium and pipetted up and down to prevent the formation of cells clump. Afterward, $10\mu\text{L}$ trypan blue was added and mixed with $10\mu\text{L}$ cell suspension on a parafilm. The mixture of cells and trypan blue was transferred to the haemocytometer by capillary action. Prior to the mixture transfer, the cover slip was wiped with 70% ethanol. The haemocytometer was transferred to inverted phase contrast microscope and viewed under 100 times magnification. The viable cells on the top and left border was counted, while the cells on the bottom and right border was excluded in counting to ensure each cells only counted once. If the cell density was too high, the cells suspension was diluted by the equation $\text{cells/mL} = A^V \times \text{DF} \times 10,000 \text{ cells/mL}$, where A^V = Average number of viable cells from 4 chambers and DF = Dilution factor.

3.5 Bioassay

3.5.1 Maximum Non Toxic Dose (MNTD) Determination by MTT assay

The cultured BV2 cells was plated at density of 1×10^4 cells per well in 100 μ l of the complete growth medium for cell attachment for one day in the humidified incubator at 37°C in 5% CO₂. On the next day, the serum-free medium was added to replace the cells and the cells growth were synchronized for another 24 hrs. On the third day, four xanthone stock solutions used were undergo two-fold dilution in DMEM medium to obtain working concentrations. Euxathone (EX) was diluted from 400 μ M - 0 μ M, while Rubraxanthone (RX) was diluted from 50 μ M - 0 μ M. For Ananixanthone (AX) and 1,3,7 trihydroxy-2,4- bis (3-methylbut-2-enyl) (TX), two-fold dilutions were performed from 300 μ M - 0 μ M. After 24 hrs incubation period the cell viability was determined by the MTT assay. Cell viability was calculated by absorbance of sample/ absorbance of control cells x 100%, while the cell cytotoxicity was calculated by 100%- cell viability %. A graph of toxicity percentage against the log₁₀ concentration of xanthenes was plotted to determine the Maximum Non Toxic Doses (MNTD), which the first x-intercept indicates toxicity is 0%.

3.5.2 Cell Viability Determination by MTT Assay

MTT 3-(4,5-dimethylthiazol-2-yl)-2,5-diphenyltetrazolium Bromide Assay viability test was used to determine the ability of natural xanthenes compound to provide neuroprotection effect against glutamate-induced cell death in BV2 microglia cells. In the assay, growth control contained only culture medium DMEM without glutamate or xanthenes. While the positive control co-

incubated with vitamin E and glutamate, and the cells with only glutamate act as negative control. The data calculated and shown in viability percentage relative to growth control. The layout of the plate was shown in Figure 3.1. A concentration of 0.5 mg/ml of MTT reagent (Calbiochem, Darmstadt, Germany) was added into each well and incubated at 37°C in CO₂ incubator for 4 hrs. Afterwards, the solution in each well was pipetted out and discarded. To solubilized the formazan crystal, 100 µL of 100% DMSO was added to each wells. The optical density of the assay was measured at wavelength 560 nm by the microplate reader.

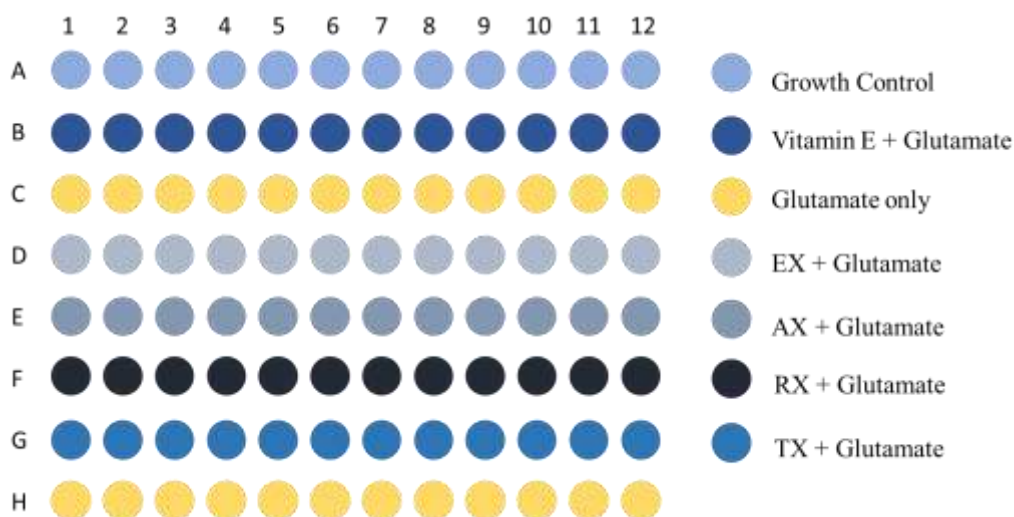


Figure 3.1: Layout of the positive control (Vitamin E + Glutamate) and negative control (Glutamate only) with co-treatment of xanthenes and glutamate

3.5.3 Intracellular Free Radical Production by DCFH-DA Assay

The intracellular reactive oxygen species produced by the BV2 cells during the co-treatment of xanthone and glutamate was determined quantitatively by DCFH-DA assay. The growth control was untreated BV2 cells with only culture medium, negative control was treated with only glutamate, while the positive control were co-treated with of glutamate and vitamin E. The layout of samples and controls is shown in Figure 3.1.

BV2 microglial cells were seeded at 10,000 cells/wells in 96-wells dark plate, and incubated in 100 μ l of complete growth medium for 24 hrs in 5% CO₂ humidified incubator at 37°C. On second day, the complete medium was replaced by serum free medium to synchronise the cell growth for next 24 hrs. On the third day, the medium in each wells was removed and washed with PBS. The procedures followed by incubation with 10 μ M of DCFH-DA (Calbiochem, Darmstadt, Germany) for 60 min in 5% CO₂ humidified incubator at 37°C. After incubation period, the DCFH-DA was removed and the cells was washed with PBS twice before incubate the cells with xanthones at MNTD and 30 mM of glutamate. The fluorescence intensity was measured by the microplate reader at 485 nm excitation wavelength and 530 nm emission wavelength. The initial reading was recorded T₀, then the fluorescence reading was recorded at 10 min, 20 min, 30 min, and at last 60 min. Each fluorescence readings from T₁₀ to T₆₀ were express relative to T₀ to obtain the changes in percentage in fluorescence intensity.

3.5.4 DAPI Nuclear Staining and Morphology Analysis

The BV2 cells followed the 4 days similar treatment procedure in section 3.3.2. After treatment, the cells were fixed in 100 μ l 4% formaldehyde for 15 mins, and followed by the morphology analysis using the inverted microscope. Afterward, the fixative formaldehyde was removed, and the cells were rinsed twice using PBS. Then, 0.2% of Triton X-100 (Thermo Scientific, Massachusetts, USA) was added and incubated for 5 mins. The cells were washed for 3 times to remove the Triton X solution prior to the cell incubation with 100 μ l of 300 nM DAPI staining reagent (Calbiochem, Darmstadt, Germany) for 15 min. After incubation period, DAPI was removed and the cells were washed 3 times before viewed under fluorescence microscope after 24 hrs at 10X. On the other hand, the apoptotic morphologies were observed by using Nikon Eclipse Ti-S Inverted microscope at 10X (Nikon instruments INC, Melvilli, New York, USA).

3.5.5 Image J Nuclear Morphology Analysis

The microscope pictures were captured by QICAM Digital CCD camera (Qimaging, Burnaby, Canada) and analysed by image J 1.37 version (NIH, USA). The images were first converted to 8-bits images, follow by auto-threshold to binary photos using the function in image J “Make Binary”. The “watershed function” was used to separate the cell nuclei, and then “Analyse Particle” function was used to determine the different morphological parameters, such as circularity, and nuclear area. The circularity formula is defined as 4π

(area/ perimeter²) in Image J. At last, the nuclear area factor (NAF) was calculated by multiplying the nuclear area with circularity (Eidet, et al., 2014).

3.6 Statistical Analysis

Student's t test was calculated using SPSS 23 (IBM, USA) and Excel (Microsoft, USA) to compare the significant difference between the growth control and glutamate treatment in order to validate the significance of using glutamate as a potent cell cytotoxic compound. While the significant difference between the glutamate treatment alone and the co-treatment of glutamate with xanthenes was calculated to determine protective effect exerted by xanthenes. The significant difference was indicated by $p < 0.05$, while $p < 0.01$ indicated there is a very significant difference.

CHAPTER 4

RESULTS

4.1 Maximum Non Toxic Dose (MNTD)

MNTD is the x- intercept in dose-dependent cytotoxic curve, which a positive cytotoxicity value indicates cell death induced by glutamate in the percentage of the cell population, while a negative cytotoxicity percentage value shows cell proliferation. Concentrations of xanthones were converted to \log_{10} concentration in dose dependent curve.

In cytotoxic curve of TX as shown in Figure 4.1 (A), the concentration above MNTD showed exponential increase in cytotoxicity percentage with slight fluctuation from concentrations 3.97 nM to 5.17 nM, while the concentration below MNTD indicated a decreased trend followed by large fluctuation from concentrations 2.46 nM to 3.07 nM. In cytotoxic curve of EX as shown in Figure 4.1 (B), the concentration above MNTD showed a smooth exponential increase in cytotoxicity percentage, while the concentration below MNTD showed a decrease trend with slight fluctuation from concentrations 2.89 nM to 3.79 nM. In cytotoxic graph of RX as shown in Figure 4.1 (C), the concentration above MNTD showed a peak increase at concentration 3.49 nM followed by a slight decrease at 3.79 nM, while the concentration below MNTD showed a slight increase trend at log concentration 2.29 nM and a large decrease trend at concentrations 2.00 nM and 0.60 nM. In cytotoxic curve of AX as shown in

Figure 4.1 (D), the concentration above MNTD showed a similar increase followed by a slight decrease at log concentration 5.18 nM, while the concentration below MNTD showed a decrease trend with a slight fluctuation from 2.46 nM to 3.67 nM respectively. In table 4.1, the highest MNTD was EX, followed by AX, RX and TX which RX showed the highest toxicity towards microglia cells as it possessed the lowest MNTD.

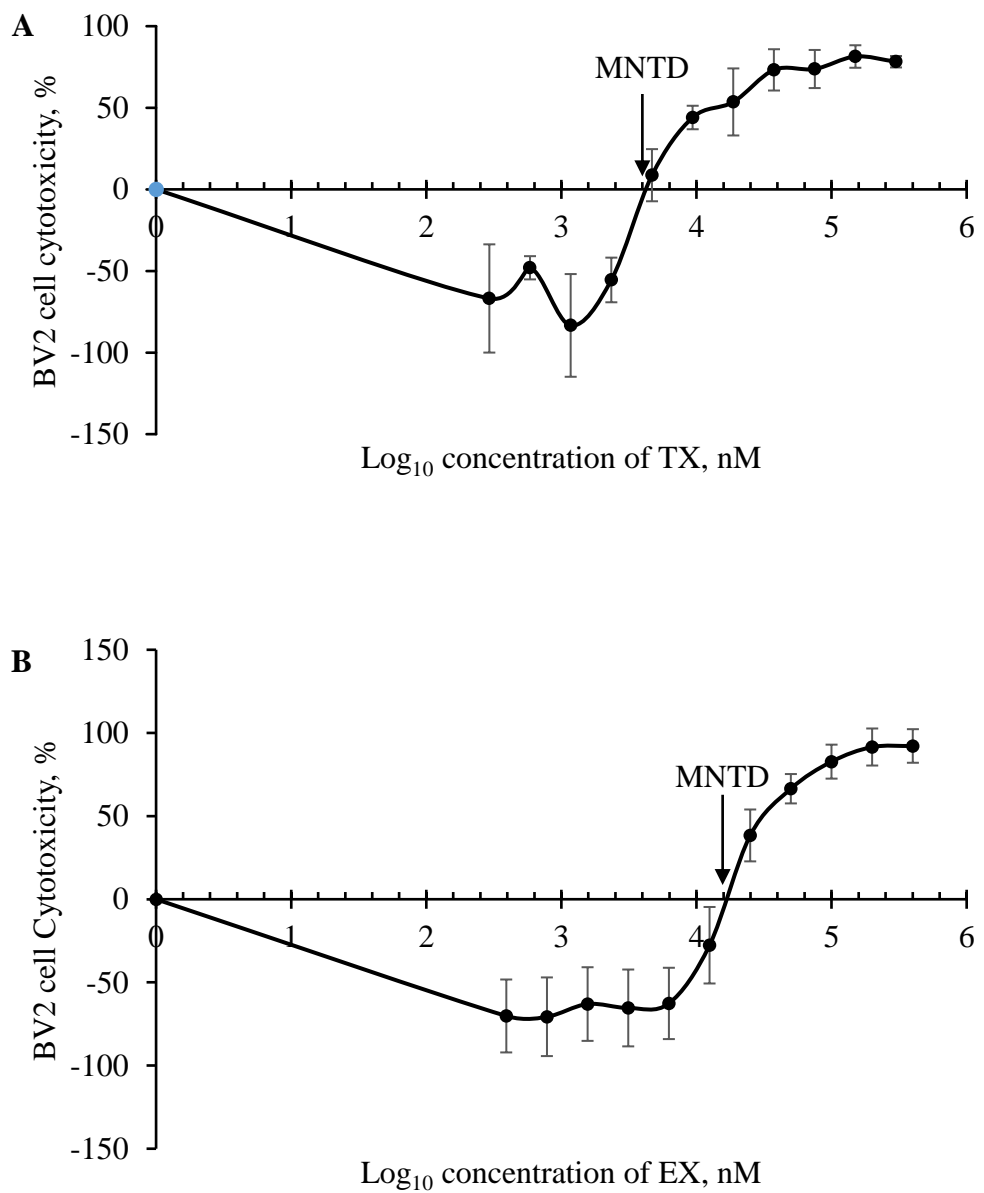


Figure legend on the next page

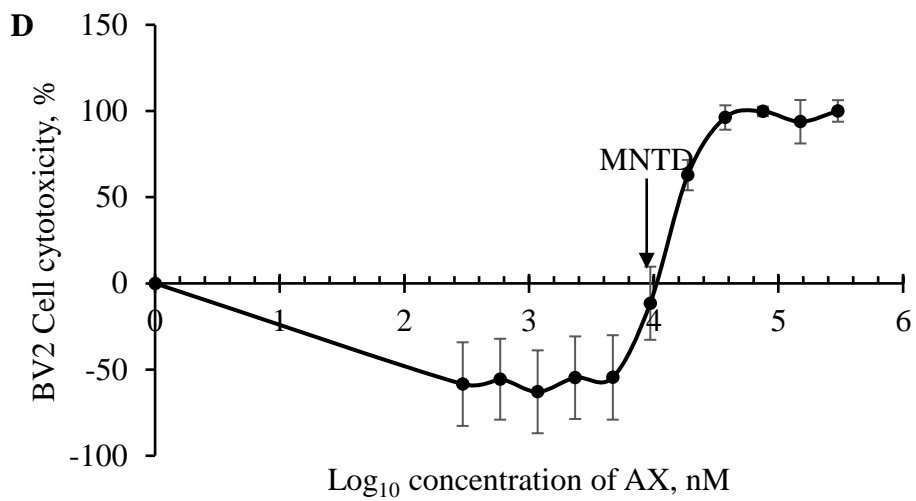
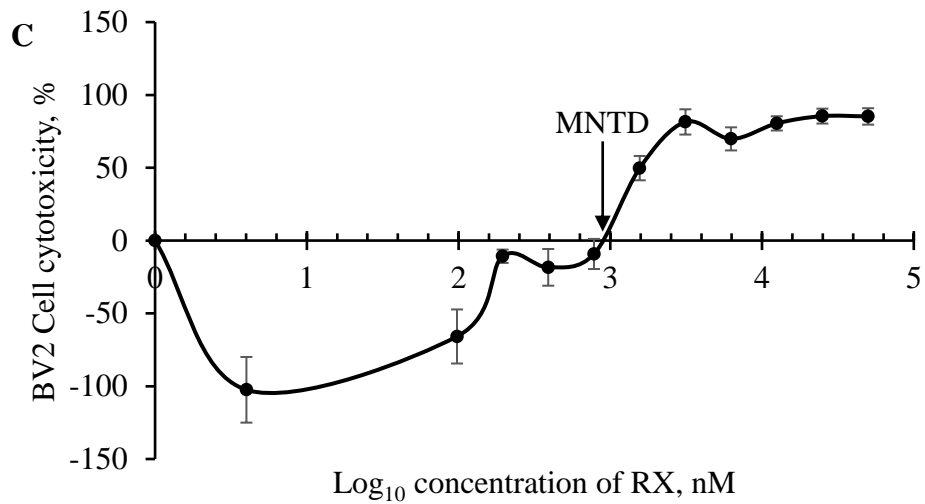


Figure 4.1: Dose-dependent BV2 cell cytotoxicity against log₁₀ concentration of (A) 1,3,7 trihydroxy-2,4- bis (3-methylbut-2-enyl) xanthone (TX), (B) Euxanthone, (C) Rubraxanthone (RX), (D) Ananixanthone (AX). Data are represented in mean \pm SEM from two independent experiments with three replicates

Table 4.1: MNTDs of the EX, RX, AX, and TX

Natural Xanthenes	MNTDs (μM)
Euxanthone (EX)	15.85
Rubraxanthone (RX)	0.89
Ananixanthone 5(AX)	10.23
1,3,7 trihydroxy-2,4- bis (3-methylbut-2-enyl) xanthone (TX)	3.98

4.2 Neuroprotection of Xanthenes in Glutamate-Induced Cell Death

As compared to growth control, glutamate treatment alone showed a significant reduction of cell viability for 33.17%. While as compared to glutamate treatment alone, co-incubation of vitamin E with glutamate showed significant increase in cell viability of BV2 cells for 27.29%. On the other hand, as compared to glutamate treatment alone, the co-treatment of EX, AX, RX and TX MNTDs with glutamate also showed significant increase in cell viability percentage. Among the four xanthenes, TX showed the most prominent effect in rescuing the BV2 cells from glutamate induced cell death, followed by RX, AX, and EX. Overall, the increase in cell viability for the four xanthenes compound showed cytoprotective potential against glutamate induced toxicity.

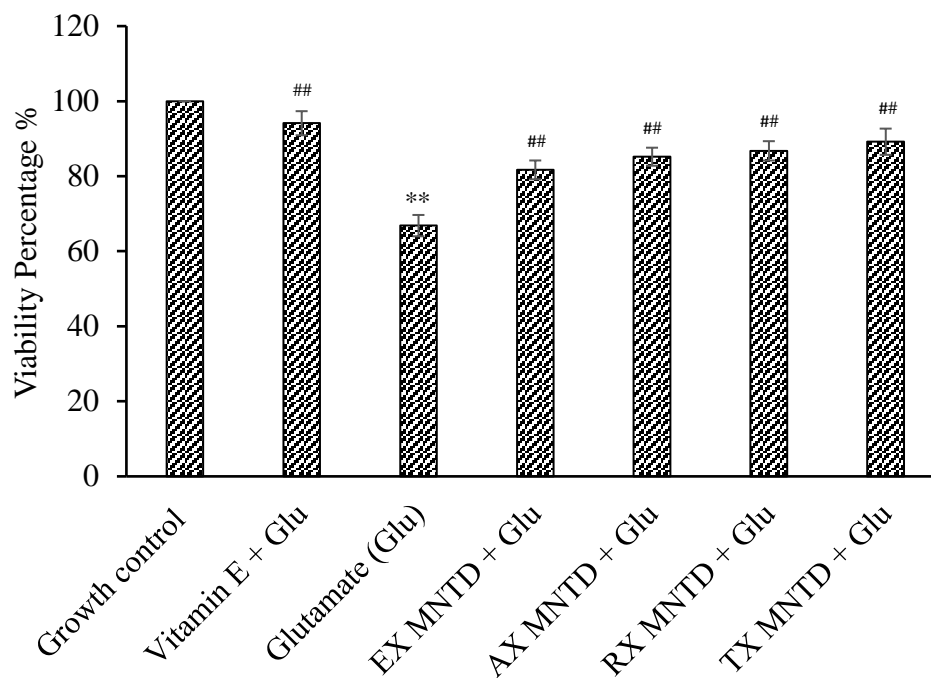


Figure 4.2: Effect of xanthenes treatment against glutamate-induced cell death on cell viability of BV2 cells. Data are presented as mean \pm SEM obtained from two independent experiment with six replicates; ** $p < 0.01$ compared to growth control while # $p < 0.05$ compared with glutamate treatment control.

4.3 DCFDA ROS Generation Test

Figure 4.3 shows the fluorescence intensity in percentage recorded at four time points at 10, 20, 30, and 60 min. Overall, the fluorescence intensity increased across 60 min. As compare to untreated growth control, glutamate treatment alone showed a significant increase in intracellular ROS at 10, 20, 30, and 60 min. As compared to glutamate treatment alone, vitamin E co-treatment with glutamate showed a mild reduction in intracellular ROS at the 10 and 20 min, followed by a slight increment at 30 min, and significant reduction at 60 min.

As compared to glutamate treatment at 10 min, RX MNTD co-treatment with glutamate showed slight increment in intracellular ROS, while EX, AX and TX

MNTD co-treatment with glutamate showed a mild reduction. As compared to glutamate treatment at 20 min, EX, AX, RX MNTD co-treatment with glutamate showed increased in intracellular ROS. While TX MNTD co-treatment with glutamate showed a marginal reduction difference, as compared to glutamate treatment alone at 20 min. At 30 min, EX, AX, and RX MNTD co-treatment with glutamate showed increase in intracellular ROS, and slight decrease in TX MNTD co-treatment with glutamate as compared to glutamate treatment control alone. At 60 min, EX, AX, RX MNTD treatment with glutamate showed a non-statistically significant reduction as compared to glutamate control, while TX showed a marginal significant reduction of intracellular ROS.

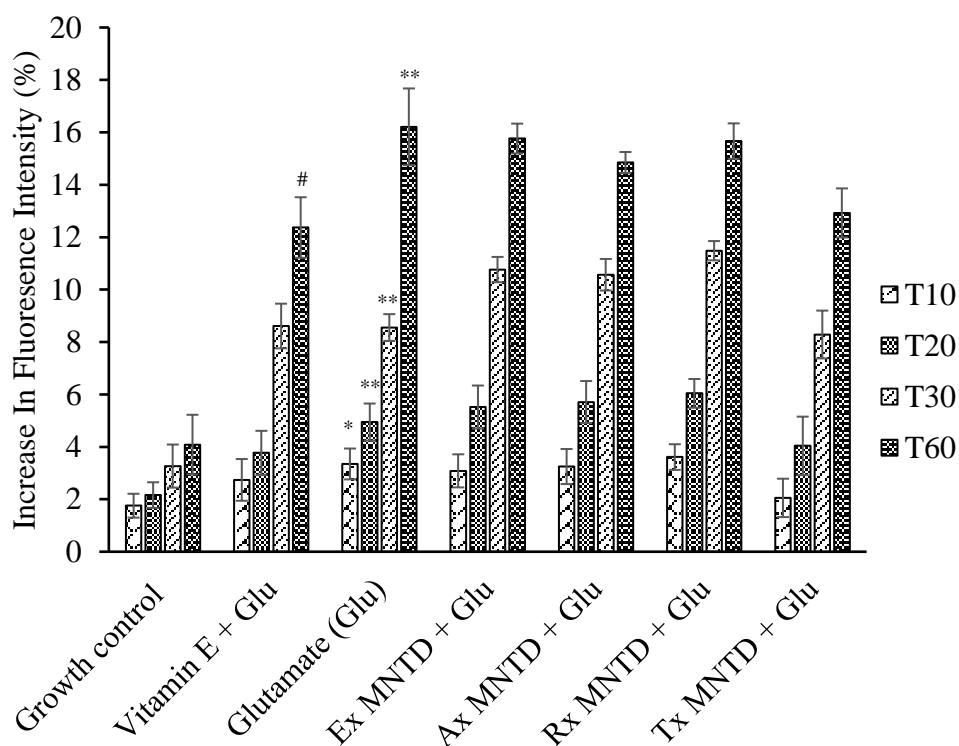


Figure 4.3: Fluorescence reading of DCFH-DA for 10, 20 30, and 60 mins. Data are presented as mean \pm SEM of two independent experiment with six replicates; * $p < 0.05$ compared to growth control while ** $p < 0.01$ compared to growth control and # $p < 0.05$ compared with glutamate treatment control.

4.4 Cells Death Morphology Analyses

4.4.1 Inverted and Fluorescence Microscope Analysis

Apoptosis characteristics like membrane blebbing and shrinkage of cells were observed using bright field microscopy, while nuclear chromatin condensation and nuclear fragmentation was observed using fluorescence microscope with DAPI-counterstained. In Figure 4.4, BV2 cells in growth control showed a round and dendritic like structure, and there is no apoptosis characteristics present in the cells. While the cells co-treatment with vitamin E and glutamate showed cells shrinkage with little chromatin condensation. BV2 cells with glutamate treatment alone showed more obvious apoptosis characteristics with cell shrinkage, large dynamic membrane blebbing, chromatin condensation and mild nuclear fragmentation. On the other hand, the cells co-treated with glutamate and EX, AX, RX, and TX showed mild cell shrinkage and chromatin condensation.

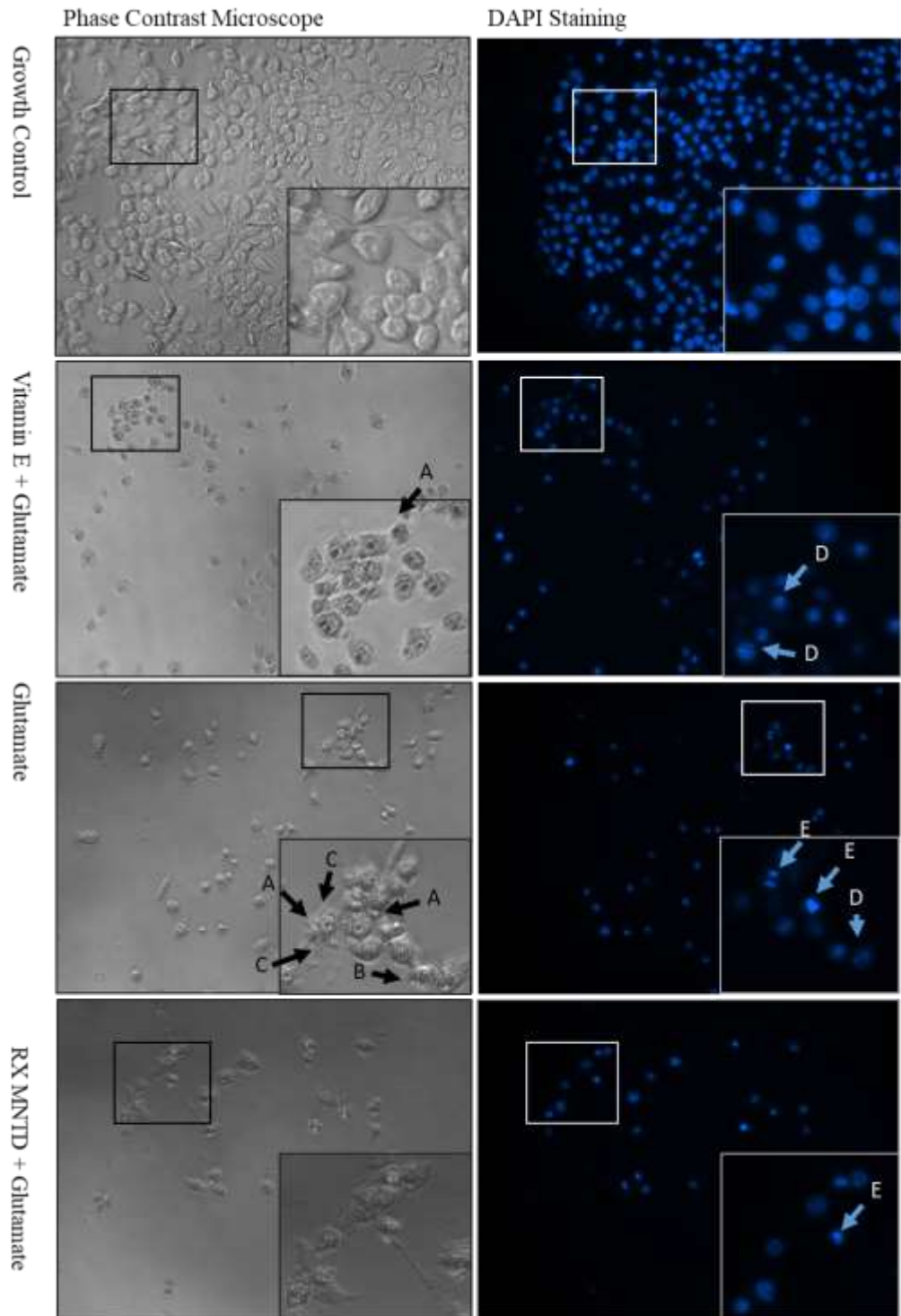


Figure legend on the next page

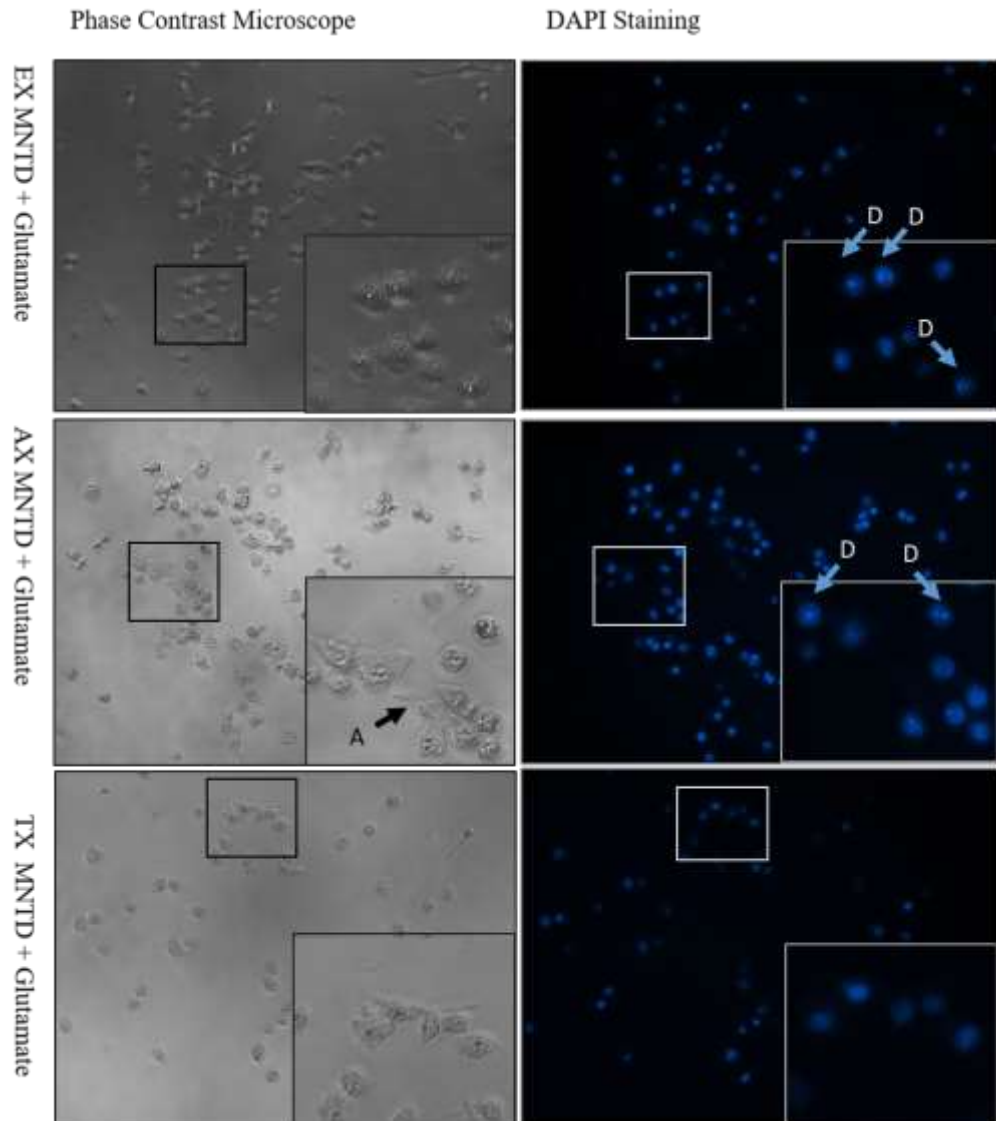


Figure 4.4: Nuclei morphological observation of BV2 cells stained with DAPI staining (blue) by fluorescence microscope for controls and xanthenes treatments (magnification 10X). Apoptosis morphology observation using bright field phase contrast inverted microscope at 10x magnification. The boxes in each figure indicated magnified region. Arrows show (A) cell shrinkage, (B) small surface membrane blebbing, and (C) large dynamic membrane blebbing, (D) Mild chromatin condensation, (E) Heavy chromatin condensation.

4.4.2 Quantification of morphological changes in nuclei

Overall, the changes of circularity between samples were not significantly different. For nuclear area, the co-treatment with MNTD of EX AX, RX, TX with glutamate prevented the shrinkage or decrease in nuclear area. The Nuclear Area Factor (NAF) for EX, AX, RX, and TX showed significant increment as compared to the glutamate treatment control. While the increment in co-treatment of vitamin E with glutamate was not statistically significant as compared to glutamate treatment control alone.

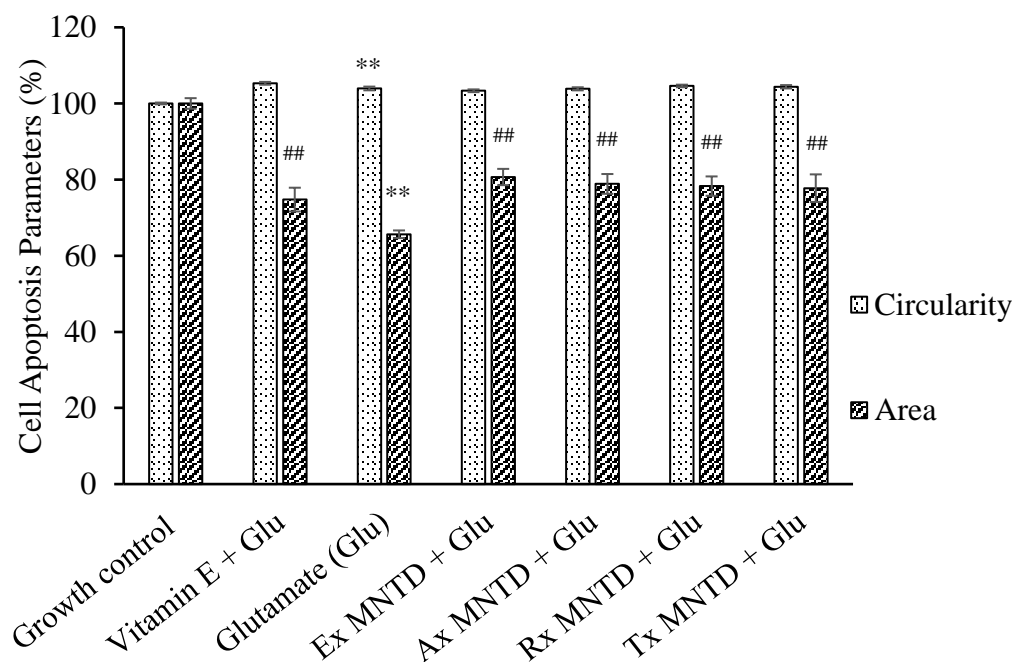


Figure 4.5: Nuclear area and circularity relative to control cells was obtained from a population of at least 15 cells. Data are presented as mean \pm SEM from two independent experiments. * $p < 0.05$ compared to growth control, while ** $p < 0.01$ compared to growth control. # $p < 0.05$ compared to glutamate control. While ## $p < 0.01$ compared to glutamate control.

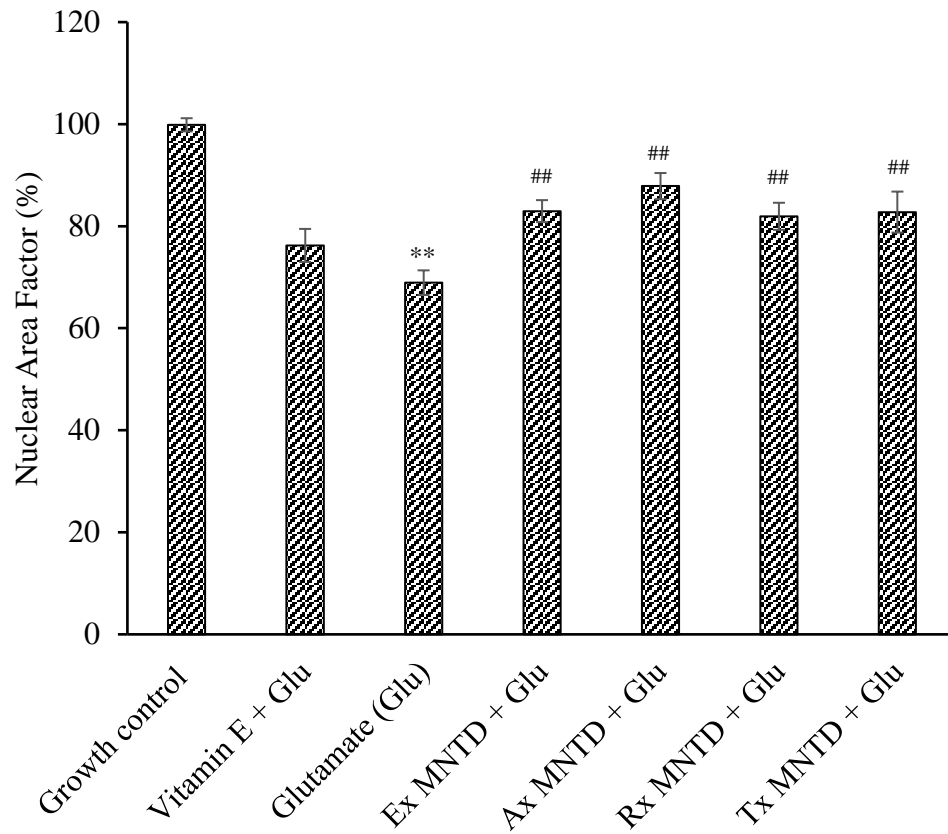


Figure 4.6: Nuclear area factor was calculated from the product of circularity and Nuclear Area. Data are presented as mean \pm SEM from two independent experiments. * $p < 0.05$ compared to growth control, while ** $p < 0.01$ compared to growth control. # $p < 0.05$ compared to glutamate control. While ## $p < 0.01$ compared to glutamate control.

CHAPTER 5

DISCUSSION

5.1 Cytotoxic Profile for EX, AX, RX, and TX

Previously, Gua Lou Gui Zhi (GLGZD), a Chinese medicine which consists of glycoside, flavonoids, and phenolic acids provided a maximum protection to BV2 cells against glutamate induced apoptosis at the concentration of 1000 $\mu\text{g/ml}$ (Li, et al., 2014). In this study, the methods used to determine the neuroprotective effect of EX, AX, RX, and TX were different. Before the determination of neuroprotective potential against the glutamate induced apoptosis, the MNTDs of four xanthenes compound were determined. MNTD determination is vital to ensure the concentration used for the following assay and treatment will not induce any toxicity to BV2 cells. The approach of using MNTD were used in neuroprotective assay for natural products like bird nest extract (Yew, et al., 2014), orientin (Law, et al., 2014), and synthetic prenylated xanthenes (Nga, et al., 2016).

In the previous research, orientin MNTD used for anti-inflammatory study against LPS induced inflammation. Orientin is a flavonoid C-glycoside which exhibits antioxidant with prominent scavenging ability. As shown in a previous study, orientin increased the level of glutathione peroxidase, catalase, and superoxide dismutase in the brain of mouse (Lam, et al., 2016). Its MNTD was determined at 15 μM in BV2 cells (Gan, et al., 2017). This result is almost

similar as compared to the MNTD of EX and AX, which is about four fold higher than MNTD of TX, and 17 fold higher than MNTD of RX. As compared to orientin, TX and AX are more toxic to BV2 cells. On the other hand, the MNTD of orientin used to study the neuroprotective properties against oxidative stress in SH-SY5Y was 20 μ M (Yew, et al., 2014), which is almost similar to the MNTD of EX, about two fold higher than the AX, fivefold higher than TX, and 22 fold higher than MNTD of RX.

The difference in the toxicity profiles of EX, AX, RX, and TX were evident in previous research, where the IC_{50} of EX against MDA-MB-231 breast adenocarcinoma, HeLA cervical adenocarcinoma, CEM-SS lymphoblastic leukaemia cells, and CaOV3 ovary adenocarcinoma were 31.9, 34.5, 27.0, and 9.0 μ g/ml respectively (Ee, et al., 2005). While the IC_{50} of AX were 4.6, > 40.0, > 40.0, and 29.7 μ g/ml for MDA-MB-231, HeLA, SEM-SS, and CaOV3 respectively (Ee, et al., 2005). On the other hand, TX showed IC_{50} at 35.6, > 40.0, > 40.0, > 40.0 for MDA-MB-231, HeLA, SEM-SS, and CaOV3 respectively (Ee, et al., 2005). For RX, the IC_{50} against CEM-SS cell line was 5.0 μ g/ml (Lee, et al., 2010). The difference in the toxicity profile may be due to the degree of cyclization of the prenyl compound and the prenylation on the xanthone (Nga, et al., 2016).

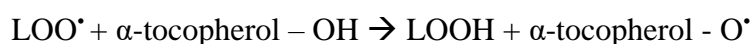
5.2 Validity of Glutamate and Vitamin E as Control Group

Glutamate alone induced 33% of significant cell death at concentration of 30 mM in BV2 cells over 24 hrs incubation. Previously, the cell death induced by glutamate in BV2 cells with the same concentration and incubation period was approximately 50% which was higher as compared to glutamate-challenge BV2 cells in this experiment (Li, et al., 2014). The difference in cell death could due to the different passage number of BV2 cells used.

High concentration of glutamate at 30 mM was used to mimic the condition after stroke, where the energy stored is loss, leading to imbalance in ionic concentration, and the release of glutamate with inhibited reuptake function. Generally, glutamate is validated as a neurotoxic inducer as it is able to induce cell death with three general mechanisms, which involves excitotoxicity, oxidative stress, and ionic imbalance (Lo, Dalkara and Moskowitz, 2003). These toxicity effects of glutamate is evident in ischemic brain injuries and stroke, which it could lead to injuries in neuron, vascular component, glia, and subcellular level like mitochondria, cell membrane, nucleus, and endoplasmic reticulum (Lo, Dalkara and Moskowitz, 2003). Besides, glutamate-activated microglia cells also express the death receptor Fas, and FasL, with the release of reactive oxygen, nitrogen species (ROS and RNS), superoxide, and proteolytic enzymes. The ROS will react with the protein, nucleic acid and lipids of neighbouring cells, and result in cellular damage (Fry, 2009).

As a lipid soluble antioxidant, vitamin E α -tocopherol was used as a positive control in the neuroprotection. In Section 4.2, α -tocopherol showed increase in cell viability percentage and reduction in intracellular ROS production as compared to glutamate treatment alone. The similar trend was also evident in a previous research which, α -tocopherol reduced 20% of the cell death induced by paraquat and 6- hydroxydopamine and decreased intracellular ROS production induced by paraquat (Nga, et al., 2016).

Vitamin E was shown able to work with glutathione (GSH) to scavenge free radicals, limits lipid peroxidation and maintains the long chain polyunsaturated fatty acid integrity in the cell membrane (Traber and Atkinson, 2007). The type of vitamin E used was α -tocopherol. It is able to act as a chain breaking antioxidant by transferring the hydrogen or sequential electron in the reaction of lipid peroxy radical (LOO^{\bullet}) with hydroxyl group as shown in equation below (Nimse and Pal, 2015):



In addition, tocopherol is also able to react with other oxygen species like singlet oxygen, peroxy nitrite, alkoxy radicals superoxide, ozone and nitrogen dioxide which further contributes its role as an antioxidant defence in the cells (Haafte, et al., 2003).

5.3 EX, AX, RX, and TX Improved Cell Viability Against Glutamate Induced Toxicity

From Section 4.2, the co-incubation of EX, AX, RX, and TX MNTD ranging from 0.89- 15.8 μM significantly prevented glutamate-induced cell death by increasing the cell viability ranging from 14% to 22%. TX had the highest protection against the glutamate induce toxicity followed by RX, AX, and EX. Among the tested natural xanthones, RX and TX are more potent neuroprotective xanthones, as they reduced glutamate induced-cell toxicity the most at a concentration as low as $< 4 \mu\text{M}$, unlike AX and EX which induced a weaker cytoprotective effect at higher concentrations $> 10 \mu\text{M}$.

Gua Lou Gui Zhi (GLCZD) decoction is a traditional medicinal herb which used for stroke treatment and neurodegenerative disease. Previously, the glutamate-induced cell death in BV2 cells was attenuated by 16.67% after GLCZD treatment at its highest concentration 1000 $\mu\text{g/ml}$ (Li, et al., 2014). As compared to RX and TX, these xanthone compounds provided higher neuroprotective effect $> 19\%$ reduction in glutamate induced-cell death with concentration $< 4 \mu\text{M}$.

On the other hand, a traditional medicine like bee venom had been used as anti-inflammatory drug to treat immune related disease such as rheumatoid arthritis. In a previous study, 2.5 $\mu\text{g/mL}$ bee venom was also able to reduce 20% cell death induced by 5 mM glutamate in BV2 cells, but 5 $\mu\text{g/mL}$ of bee venom did not show protective effect against glutamate toxicity (Lee, et al., 2012). However, in this study, the MNTD of TX showed higher neuroprotective effect

which it was able to attenuate 22.34% cell death when incubated with 30 mM glutamate after 24 hrs.

Overall MTT assay revealed that glutamate control treatment increases apoptosis events, and the four tested xanthone compound can reduce apoptosis. Among all the xanthenes, TX showed the best neuroprotective effect against glutamate induced cell death. As compared to GLCZD (Li, et al., 2014) and bee venom (Lee, et al., 2012), TX also showed a higher neuroprotective activity. In MTT assay results, BV2 cells co-treated with xanthone compounds and glutamate protects the function of mitochondrial dehydrogenase in BV2 cells which will convert the water- soluble tetrazolium dye from yellow to purple formazan (Riss, et al., 2013). However, the detailed cytoprotective mechanism of xanthenes is still inconclusive with only results from MTT assay, Hence, the intracellular ROS level was measured to determine the free radical scavenging activity against glutamate-induced cell death.

5.4 EX, AX, RX, and TX Did Not Attenuate ROS in Glutamate-Challenged BV2 cells

Intracellular ROS measurement is vital to determine the oxidative stress level in the cells. Oxidative stress is an important factor which causes neurodegenerative diseases. As ROS accumulates in the cells, the damage of lipid, DNA, and protein often occurs (Bagli, et al., 2016).

From results in Section 4.3, glutamate treatment control showed the highest intracellular ROS level of 16.12% at 60 min. The increment in ROS production could be due to the mechanism involving glutamate/cysteine antiporter system. In high glutamate extracellular environment, cysteine influx is blocked by the gradient driven-glutamate/cysteine antiporter system X_c^- . Therefore, the low cysteine level halts intracellular GSH synthesis. Hence, GSH level is depleted and unable to remove the reactive oxygen species (ROS), which eventually causes oxidative stress and cell death in glutamate-challenged cells (Lewerenz, Klein and Methner, 2006). In a previous study, intracellular ROS increased to 290% after stimulation with 5 mM of glutamate for 30 min in PC12 cells (Olatunji, Chen and Zhou, 2016). The difference between the elevated level of ROS may due to the different cell line used. Furthermore, in microglia cells like BV2, there are opposing actions in microglial group I receptors mGluRs, such as mGluR1 α and mGluR5. When both receptors are activated in microglia activation, mGluR1 α will promote the release of ROS and NO, while the mGluR5 will decrease the ROS and NO. Hence this might result in a lower ROS production as compared to the ROS level produced by other cell lines (Fry, 2009).

At 10, 20, 30 mins, the treatment of glutamate with EX, AX, RX indicated a higher level of intracellular level of ROS as compared to glutamate control, but the ROS level was reduced to a level lower than glutamate treatment control at 60 min. Although the reduction level of ROS did not reach statistical significance, but the trend might suggest that EX, AX, and RX may require more time to exert their antioxidant effect.

As compared to glutamate treatment alone, co-treatment of TX and glutamate had a lower ROS level at 10 and 30 min, while at 60 min there was a marginal significant reduction. Overall there was no significant attenuation in the ROS production in all xanthenes treatment as compared to glutamate treatment alone, which this may indicate there are different mechanisms involved in promoting cell viability in MTT assay. Similarly, the ROS attenuation mechanism also was not shown in the co-treatment of S1 edible bird nest MNTD and OHDA-6 (Yew et al., 2014). Although there were a few studies which revealed xanthone compound have antioxidant potential in xanthenes extracted from mangosteen peel extract (Suttirak and Manurakchinakorn, 2014; Kondo, et al., 2009; Thong, et al., 2015), but there were also investigations which found that the polyphenol compounds including xanthenes showed dual behaviour of antioxidant and pro-oxidant (Chitchumroonchokchai, et al., 2012). These compounds exhibit antioxidant activities mainly by donating hydrogen atom but in some circumstances this will result in the formation of another radical with the O-H group in the phenolic compound. Although the radicals were formed, but they exert less effect than the previous one (Information Resources Management Association USA, 2018). Overall, xanthone compounds did not show significant reduction in the ROS level in this study.

The result of rescued cell viability in MTT assay with a non-significant ROS reduction might indicate there are other mechanisms involved in cytoprotective protection. The hypothesized cytoprotective mechanism involves glutamate metabolism in microglia, as from previous research showed excitatory amino acid transporter gene EAAT-1 and EAAT-2 are present in microglial cells of mice or macaques (Lee, et al., 2012). The uptake of glutamate through EAAT-

1 and EAAT-2, followed by metabolism from glutamate to glutamine in microglia cells is similar to the mechanism of astrocyte (Lee et al., 2012). As the glutamate uptake occurs, it is able to buffer and reduce extracellular glutamate, prevent the binding of glutamate to group II mGluR and eventually rescue the cells from glutamate-induced apoptosis (Fry, 2009).

5.5 EX, AX, RX, and TX Prevent Glutamate-induced Apoptotic Changes in BV2 cells

From the morphology of BV2 growth control cells, the structure resembles amoeboid shape with long projection. The microglia cell in the normal healthy central nervous system *in vivo*, and the microglial structure *ex vivo* are different. In central nervous system, resting microglia are in ramified structure. This ramified microglia cells may transform into an amoeboid phagocytic structure when encounter with the subtle microenvironment changes like injury, stress, and pathogens invasion (Ferreira and Bernardino, 2015). However, *ex vivo* microglia cells do not show a highly ramified structure but the structure resemble amoeboid shape with projection which the structure transformation may result from the isolation process itself (Ferreira and Bernardino, 2015). Therefore, in BV2 cell culture, the resting amoeboid shape cell with some projection is less distinguishable from the activated form of microglia cell culture. Hence, the morphology analysis is mainly focused on the apoptotic structural changes like degree of membrane blebbing, and nuclear condensation.

From the morphology observation of BV2 cells in glutamate treatment alone, the nuclei were highly condensed with large dynamic cell membrane blebbing. These morphological observations indicate the cells were in early apoptosis process, which is characterized by chromatin condensation and plasma membrane blebbing. While late apoptosis characteristics like karyorrhexis and the formation of apoptotic bodies are less evident in the microglia structural observation (Elmore, 2007). Besides, the co-treatment of xanthenes or vitamin E with glutamate showed mostly mild chromatin condensation and lesser cell shrinkage. This observation supports the rescued cell viability in Section 4.1, where there were lesser cells undergoing apoptosis, however further determination of cells apoptosis was confirmed by quantification of nuclear morphology and nuclear area factor.

5.6 EX, AX, RX, and TX Rescued BV2 Cells Nuclei Apoptotic Progression

Apoptotic morphology characteristics like nuclear area and circularity can act as indicator of programmed cell death activation (Eidet, et al., 2014). BV2 cells with glutamate treatment alone had the lowest nuclear area, while with addition of xanthone treatment, the cells had higher nuclear area. The lower nuclear area measurement indicates that the nucleus undergoes early degeneration. This characteristic only occurs in apoptotic cells but not necrotic cells, as during necrosis the cell's nucleus is intact (Eidet, et al., 2014).

In term of nuclear circularity, there was insignificant difference between the glutamate control group and xanthone-glutamate co-treated group, as the nuclear fragmentation was less evident, and less proportion of cells progressed to late apoptosis. Furthermore, both nuclear area and circularity are important in the calculation of nuclear area factor (NAF), which is defined as nuclear area multiple by the circularity. NAF was used previously to determine the apoptosis of hepatic carcinoma-treated cell line. The result showed decrease in the NAF as the concentration of dehydrogenase inhibitor gossypol increased from 50 μ M to 100 μ M in the Hep-2 squamous hepatic carcinoma cell lines (Nermeen, et al., 2012).

In this study, NAF in the glutamate treatment alone was the lowest, indicating there was apoptosis progression. While in all the xanthenes co-treatment with the glutamate, NAF was significantly higher than the glutamate treatment alone. These higher NAF values correspond with the increased cell viability and less apoptotic changes in morphological observation. Therefore, EX, AX, TX, RX, and TX showed their cytoprotective effect against glutamate induced cell death, although the detailed cytoprotective mechanism of action is still inconclusive.

5.7 Limitations of Study

5.7.1 *In vitro* Studies Not Necessarily Reflective of *in vivo* Clinical Studies

In vitro cell line had been useful in predicting and determining preliminary clinical response, but the drug interaction and bioavailability still require confirmation by *in vivo* studies. The neuroprotective response showed in *in vitro* studies does not represent or show completely similar effect in *in vivo* studies (Niu and Wang, 2015). Furthermore, clinical subject might responded to xanthone differently, due to the germline and somatic genetic variation in the host of study. In addition, pharmacokinetics and pharmacodynamics of xanthenes compound were not studied in this experiments. Xanthenes might be removed or metabolized when they enter *in vivo* system. Most often the xenobiotics enter the body undergo absorption, distribution, metabolism and excretion, which these processes may affect the bioavailability of the xanthenes in the body (Jaroch, Jaroch and Bojko, 2018).

Besides, *in vitro* microglial culture is usually grown in serum, which it might induce the gene expression to mimic the activated microglial form. However, the serum-induced gene expression effect will not be shown in *in vivo* system, as the cell resident in CNS are not exposed to serum, therefore some gene expression might not be activated in an *in vivo* system (Howe and Barres, 2012).

5.7.2 Microglia Culture Less Representative the Neuron-glia Interaction

In glia-neuron co-culture system, both glia and neuronal cells also will interact with one another in neurotoxicity and neuroprotection microenvironment. For instance, the high A β does not cause damage to the neuronal culture cells, but when co-cultured with microglia cells, there is a significant increment in the tau protein phosphorylation and formation of tangles (Mhatre, et al., 2015). Besides, in term of microglia activation, the suppression of microglia at M1 phase and reduction in ROS release was shown only in the co culture of the microglia cells with motor neurons in the presence of IL-4. Hence, neuroprotective effect evaluation with only the microglial cell in absence of neurons in this experiment settings might be insufficient to represent the effect in CNS system (Neiva, et al., 2014).

5.7.3 Inconsistency in Experiment

The inconsistency might result from different technical procedure used in preparation of experiment (Stansley, Post and Hensley, 2012). For instances, inconsistency of result have been shown previously, which Cheepsunthorn et al (2001) discovered both the TNF expression and release increase in HAPI microglia cells after LPS stimulation, but in Horvath et al (2009) study, only the TNF expression was increased, but not the TNF release. Furthermore, *in vitro* microglial response in the immortalized cell lines may become weaker as the passage number becomes higher (Ferreira and Bernardino, 2015). These

immortalized cell line may undergo genetic drift or selection for certain phenotype as the passage number increase (Stansley, Post and Hensley, 2012).

5.8 Further Studies

Besides using glutamate as a neurotoxin model, there are other neuropathological causative agents such as A β in Alzheimer's, and 6-hydroxydopamine (6-OHDA) in Parkinson's disease (Bové and Perier, 2012). The results in this experiment indicated EX, AX, RX, and TX did exert glia-protection against glutamate induced cell death, although the ROS reduction was not significant. Hence, further study in the role of glutamine-glutamate metabolism in glial-protection mechanism is required. Besides, the neuronal-glial interaction should also be investigated to complete the neuroprotection and glial-protection mechanism of xanthones.

Furthermore, the role of glutamate transporter should also be investigated in the study of glia protection mechanism, as high extracellular glutamate can cause oxidative stress and excitotoxicity, therefore uptake of glutamate by EAAT1 and EAAT 2, followed by metabolism it into glutamine is vital to reduce the extracellular glutamate level. In pathological conditions like Alzheimer's disease (AD), multiple sclerosis and experimental autoimmune encephalomyelitis, the decrease in expression of excitatory amino acid transporter EAAT1 and EAAT2 were reported, which leads to lesser uptake of glutamate and further contribute to the glutamate-induced toxicity (Fry, 2009). Therefore, the cytoprotection mechanism can be studied via the expression level

of EAAT1 and EAAT 2 to further identify whether the xanthone treatment induces increase in glutamate uptake. On the other hand, to confirm the involvement of glutamate-glutamine metabolism, the expression level of glutamine synthetase can also be targeted for subsequent gliaprotection study (Lee, et al., 2012).

In addition, there are some modifications and improvement on the experiment settings. First, apoptotic gene expression study such as Bcl/Bax and caspases-3 should be included in the experimental setting to confirm MTT results and apoptosis progression. Then, induction of apoptosis also can be evaluated by mitochondrial membrane potential (MMP) assay, as the mitochondrial permeability transition pore opening will induce depolarization of transmembrane potential and result in loss of oxidative phosphorylation and release of apoptotic factors.

CHAPTER 6

CONCLUSIONS

In conclusion, the maximum non-toxic dose (MNTD) of natural xanthone compounds EX, AX, RX, and TX towards BV2 microglial cell line were 15.85 μM , 10.23 μM , 0.89 μM , and 3.98 μM respectively, which RX showed the highest toxicity towards microglia cells as it possessed the lowest MNTD. From MTT cell viability test, all the xanthenes compounds showed a significant cytoprotective effect against glutamate-induced toxicity. Among the four xanthenes, TX showed the highest glia-protective effects followed by RX, AX, and EX. All xanthenes did not attenuate glutamate-induced ROS generation in the BV2 cells, although there was a marginal reduction in ROS level in the co-treatment of TX and glutamate at 60 min. Furthermore, the mode of cell death was determined to be apoptosis, where there are observable membrane blebbing and nuclear condensations. The apoptotic progress indicated the cells undergo early apoptosis when treated with high concentration of glutamate. In addition, the cytoprotective effect was further confirmed by the nuclear area factor (NAF) measurement, where all the NAF value in the co-treatment of xanthone and glutamate indicated a lesser apoptotic progression in the cells as compared to glutamate treatment alone. To conclude, rescued cell viability, higher NAF, lesser apoptotic progression showed xanthenes provided cytoprotective effect but the non-significant reduction in ROS generation indicated that there are

other mechanisms such as glutamate-glutamine metabolism involved in the cytoprotection mechanism instead of ROS reduction mechanism.

REFERENCES

- Antala, B., Buhva, S., Gupta, S., Lakhar, M., Patal, M. and Rabadiya, S., 2012. Protective effect of methanolic extract of *Garcinia indica* fruits in 6-OHDA rat model of Parkinson's disease. *Indian Journal of Pharmacology*, 44(6), p. 683.
- Bagli, E. Goussia, A., Moschos, M.M., Agnantis, N. and Kitsos, G., 2016. Natural compounds and neuroprotection: Mechanisms of action and novel delivery systems. *In Vivo*, 30(5), pp. 535–547.
- Begni, B., Brighina, L., Sirtori, E., Fumagalli, L., Andreoni, S., Beretta, S., Oster, T., Malaplate, A.C., Isella, V., Appollonio, I. and Ferrarese, C., 2004. Oxidative stress impairs glutamate uptake in fibroblasts from patients with Alzheimer's disease. *Free Radical Biology & Medicine*, 37(6), pp. 892–901.
- Beneyto, M., Kristiansen, L.V., Oni, O.A., McCullumsmith, R., Meador, W., James, H., 2007. Abnormal glutamate receptor expression in the medial temporal lobe in schizophrenia and mood disorders. *Neuropsychopharmacology*, 32(9), pp. 1888–1902.
- Birben, E., Sahiner, U.M., Sackesen, C., Erzurum, S. and Kalayci, O., 2012. Oxidative stress and antioxidant defense. *The World Allergy Organization Journal*, 5(1), pp. 9–19.
- Bové, J. and Perier, C., 2012. Neurotoxin-based models of Parkinson's disease. *Neuroscience*, 2(11) pp. 51–76.
- Brown, G.C., 2007. Nitric oxide and mitochondria. *Frontiers in Bioscience : Journal and Virtual Library*, 12(2), pp. 1024–1033.
- Brown, G.C. 2010. Nitric oxide and neuronal death. *Nitric oxide : Biology and Chemistry / Official Journal of the Nitric Oxide Society*, 23(3), pp. 153–165.
- Câmara, D.V., Lemos, V.S., Santos, M.H., Nagem, T.J. and Cortes, S.F., 2010. Mechanism of the vasodilator effect of Euxanthone in rat small mesenteric arteries. *Phytomedicine*, 17(8–9), pp. 690–692.

Chen, Z. and Trapp, B.D., 2016. Microglia and neuroprotection. *Journal of Neurochemistry*, 136(1), pp. 10–17.

Chitchumroonchokchai, C., Riedl, K.M., Suksumrarn, S., Clinton, S.K., Kinghorn, A.D. and Failla, M.L., 2012. Xanthones in mangosteen juice are absorbed and partially conjugated by healthy adults. *Journal of Nutrition*, 142(4), pp. 675–680.

Domercq, M., Vázquez, V.N. and Matute, C., 2013. Neurotransmitter signaling in the pathophysiology of microglia. *Frontiers in Cellular Neuroscience*, 7(49), pp. 1-11.

Du, X.G., Wang, W., Zhang, S.P., Pu, X.P., Zhang, Q.Y., Ye, M., Zhao, Y.Y., Wang, B.R., Khan, I.A. and Guo, D.A., 2010. Neuroprotective xanthone glycosides from *Swertia punicea*. *Journal of Natural Products*, 73(8), pp. 1422–1426.

Ee, G.C., Lim, C.K., Rahmat, A. and Lee, H. L., 2005. Cytotoxic activities of chemical constituents from *Mesua daphnifolia*. *Tropical Biomedicine*, 22(2), pp. 99–102.

Ee, G.C., Izzaddin, S.A., Rahmani, M., Sukari, M.A. and Lee, H. L., 2006. γ -mangostin and rubraxanthone, two potential lead compounds for anti-cancer activity against CEM-SS cell line. *Natural Product Sciences*, 12(3), pp. 138–143.

Ee, G.C.L., The, S.S., Mah, S.H., Jamaluddin, N.J., Muhamad S.M., Ahmad, Z., 2015. Acetyl-cholinesterase enzyme inhibitory effect of calophyllum species. *Tropical Journal of Pharmaceutical Research*, 14(11), pp. 2005–2008.

Eidet, J.R., Pasovic, L., Maria, R. Jackson, C.J. and Utheim, T.P., 2014. Objective assessment of changes in nuclear morphology and cell distribution following induction of apoptosis. *Diagnostic Pathology*, 9(1).

Elmore, S. 2007. Apoptosis: A Review of Programmed Cell Death, *Toxicologic Pathology*, 35(4), pp. 495–516.

Ferreira, R. and Bernardino, L. 2015. Dual role of microglia in health and disease: pushing the balance toward repair. *Frontiers in Cellular Neuroscience*, 9(51), pp. 1-2.

Fouotsa, H., Lannang, A.M., Dzoyem, J.P., Tatsimo, S.J.N., Neumann, B., Mbazoa, C.D., Razakarivony, A., Andriamarolahy, N., Augustin E., Eloff, J. N. and Sewald, N., 2015. Antibacterial and antioxidant xanthenes and benzophenone from *Garcinia smeathmannii*. *Planta Medica*, 81(7), pp. 594–599.

Fry, V.A.H., 2009. *Microglial Glutathione and Glutamate: Regulation Mechanisms*. London: University of London.

Gan, P.H., Pick, A.K.L., Gah, K.L.V., Rhun, Y.K. and Ying, P.W., 2017. Investigation anti-inflammatory mechanism of the orienting in lipopolysaccharides-induced BV2 microglia cells. *ISER 65 th International Conference on Science, Helth and Medicine*. Singapore, 2-3 July 2017.

Gopalakrishnan, G., Banumathi, B. and Suresh, G. 1997. Evaluation of the antifungal activity of natural xanthenes from *Garcinia mangostana* and their synthetic derivatives. *Journal of Natural Products*, 60(5), pp. 519–524.

Haafte, V., Rachel I. M., Haenen, G.M., Evelo, C.A. and Bast, A., 2003. Effect of vitamin E on glutathione-dependent enzymes. *Drug Metabolism Reviews*, 35(2–3), pp. 215–253.

Harrigan, T.J., Abdullaev, I.F., Jourdeuil, D. and Mongin, A.A., 2008. Activation of microglia with zymosan promotes excitatory amino acid release via volume-regulated anion channels: The role of NADPH oxidases. *Journal of Neurochemistry*, 106(6), pp. 2449–2462.

Harvey, A.L. and Cree, I.A., 2010. High-throughput screening of natural products for cancer therapy. *Planta Medica*, 76(11), pp. 1080–1086.

Harvey, B.H. and Shahid, M. 2012. Metabotropic and ionotropic glutamate receptors as neurobiological targets in anxiety and stress-related disorders: Focus on pharmacology and preclinical translational models. *Pharmacology Biochemistry and Behavior*, 100(4), pp. 775–800.

Haslund, V.J., McBean, G., Jaquet, V. and Vilhardt, F., 2016. NADPH oxidases in Microglia oxidant production: activating receptors, pharmacology, and association with disease. *British Journal of Pharmacology*, 174(12), pp. 1733–1749.

Howe, M. L. and Barres, B.A. 2012. A novel role for microglia in minimizing excitotoxicity. *BMC Biology*. 10(7), pp. 1-3.

Information Resources Management Association., 2018. *Food Science and Nutrition: Breakthroughs in Research and Practice: Breakthroughs in Research and Practice*. United States of America: IGI Global.

Jantan, I., Pizar, M.M., Idris, M.S., Taher, M. and Ali, R.M., 2002. In vitro inhibitory effect of rubraxanthone isolated from *Garcinia parvifolia* on platelet-activating factor receptor binding. *Planta Medica*, 68(12), pp. 1133–1134.

Jaroch, K., Jaroch, A. and Bojko, B. 2018, Cell cultures in drug discovery and development: The need of reliable in vitro-in vivo extrapolation for pharmacodynamics and pharmacokinetics assessment. *Journal of Pharmaceutical and Biomedical Analysis*, 147 pp. 297–312.

Kaur, C., Sivakumar, V., Ang, L. and Sundaresan, A., 2006. Hypoxic damage to the periventricular white matter in neonatal brain: Role of vascular endothelial growth factor, nitric oxide and excitotoxicity. *Journal of Neurochemistry*, 98(4), pp. 1200–1216.

Kawakami, S.K., Gledhill, M. and Achterberg, E.P. 2006. Production of phytochelatins and glutathione by marine phytoplankton in response to metal stress. [Photograph] *Journal of Phycology*, pp. 975–989.

Kondo, M., Zhang, L., Ji, H.P., Kou, Y. and Ou, B., 2009. Bioavailability and antioxidant effects of a xanthone-rich mangosteen *Garcinia mangostana* product in humans. *Journal of Agricultural and Food Chemistry*, 57(19), pp. 8788–8792.

Kumar, G.P and Khanum, F., 2012. Neuroprotective potential of phytochemicals *Pharmacognosy Reviews*, 6(12), p. 81.

Kwon, J.Y., Hiep, N.T., Kim, D.W., Hwang, B.Y., Lee, H.J., Mar, W.C. and Lee, D.H., 2014 Neuroprotective xanthones from the root bark of *Cudrania tricuspidata*. *Journal of Natural Products*, 77(8), pp. 1893–1901.

Lam, K.Y., Ling, A.P.K., Koh, R.Y., Wong, Y.P., and Say, Y.H., 2016. A review on medicinal properties of orientin. *Advances in Pharmacological Sciences*, 2016(2016), pp. 1-9.

Law, B.J.T., Ling, A.P.K., Koh, R.Y., Chye, S.M. and Wong, Y.P., 2014. Neuroprotective effects of orientin on hydrogen peroxide-induced apoptosis in SH-SY5Y cells. *Molecular Medicine Reports*, 9(3), pp. 947–954.

Lee, K.W., Zamakshshari, N.H., Ee, C.L., Mah, S.H. and Mohd Nor, S.M., 2017. Isolation and structural modifications of ananixanthone from *Calophyllum teysmannii* and their cytotoxic activities. *Natural Product Research*. Taylor & Francis, 6419(8), pp. 1–5.

Lee, S.M., Yang, E.J., Choi, S.K., Kim, S.H., Baek, M.G. and Jiang, J.H., 2012. Effects of bee venom on glutamate-induced toxicity in neuronal and glial cells. *Evidence-based Complementary and Alternative Medicine*, 2012(1), pp. 1-9.

Lee, Y.B., Ko, K.C., Shi, M.D., Liao, Y.C., Chiang, T.A., Wu, P.F., Shih, Y.X. and Shih, Y.W., 2010. Alpha-Mangostin, a novel dietary xanthone, suppresses TPA-mediated MMP-2 and MMP-9 expressions through the erk signaling pathway in mcf-7 human breast adenocarcinoma cells. *Journal of Food Science*, 75(1), pp. 13-21.

Lewerenz, J., Klein, M. and Methner, A., 2006. Cooperative action of glutamate transporters and cystine/glutamate antiporter system Xc-protects from oxidative glutamate toxicity. *Journal of Neurochemistry*, 98(3), pp. 916–925.

Li, Z.F., Hu, H.X., Lin, R.H., Mao, J.J., Zhu, X.Q., Hong, Z.F., Tao, J., Zhang, Y. and Chen, L.D., 2014. Neuroprotective effects of Gua Lou Gui Zhi decoction against glutamate-induced apoptosis in BV-2 cells. *International Journal of Molecular Medicine*, 33(3), pp. 597–604.

Liu, H., Leak, R.K. and Hu, X., 2016. Neurotransmitter receptors on microglia. *Stroke Vascular Neurology*, 1(2), pp. 52-58.

Lo, E.H., Dalkara, T. and Moskowitz, M.A., 2003. Neurological diseases: Mechanisms, challenges and opportunities in stroke. *Nature Reviews Neuroscience*, 4(5), pp. 399–414.

Mallick, H.N., 2007. Understanding safety of glutamate in food and brain. *Indian Journal of Physiology and Pharmacology*, 51(3), pp. 216–234.

Machmudah, S., Yasa, Q., Shididiqi, A., Kharisma, A.D., Widiyasuti, W., Kanda, H., Winardi, S. and Goto., M., 2015. Subcritical water extraction of xanthone from mangosteen (*Garcinia Mangostana Linn*) pericarp. [photograph] *Journal of Chemical Engineering*. 5(1), pp. 1-8.

Minikel, E., 2015. *Peroxynitrite*. [electronic print] Available at: <<http://www.cureffi.org/2015/04/30/how-do-sod1-mutations-cause-als/>> [Accessed 8 April 2018].

Mhatre, S.D., Tsai, C.A., Rubin, A.J., James, M.L. and Andreasson, K.I., Microglial Malfunction: The third rail in the development of alzheimer's disease. *Trends in Neurosciences*, 38(10), pp. 621–636.

Mark, L.P., Prost, R.W., Ulmer, J.L., Smith, M.M., Daniels, D.L., Strottmann, J.M., Brown, W.D. and Hacin, L., 2001. Pictorial review of glutamate excitotoxicity: Fundamental concepts for neuroimaging. *American Journal of Neuroradiology*, 22(10), pp. 1813–1824.

Martinez, A., Marin, E. H. & Galano, A., 2012. Xanthone as antioxidants: A theoretical study on the thermodynamics kinetics of the single electron transfer mechanism. *Food and Function*, 3(1), pp. 442-450.

Mattson, M.P. and Magnus, T., 2006. Ageing and neuronal vulnerability. *Nature Reviews Neuroscience*, 7(4), pp. 278–294.

Matute, C., Domercq, M. and Sanchez-Gomez, M.V., 2006. Glutamate-mediated glial injury: mechanisms and clinical importance. *Glia*, 53(2), pp. 212–224.

National Museum of Natural History Collections, 2018. *Calophyllum antillanum*. [photograph] Smithsonian Institution.

National Parks Board, 2013. *Garcinia parvifolia*. [photograph] National Parks Board.

Nai-Ki, M., Li, W. K., Zhang, M., Wong, R.N.K., Tai, L.S., Yung, K.K.L. and Leung, H.W., 1999. Effects of euxanthone on neuronal differentiation. *Life Sciences*, 66(4), pp. 347–354.

Naidu, M., Kuan, C.Y.K., Lo, W.L., Raza, M., Tolkovsky, A., Mak, N.K., Wong, R.N.S. and Keynes, R., 2007. Analysis of the action of euxanthone, a plant-derived compound that stimulates neurite outgrowth. *Neuroscience*, 148(4), pp. 915–924.

Negi, J.S., Bisht, V.K., Singh, P. Rawat, M.S.M. and Joshi, G.P., 2013. Naturally occurring xanthenes: Chemistry and Biology. *Journal of Applied Chemistry*, 2013(1), pp. 1–9.

Nermeen , S.A., Ehab, S.A.H., Houry, M.B. and Ali, F.M., 2012. Nuclear area factor as a novel estimate for apoptosis in oral squamous cell carcinoma - Treated Cell Line: A comparative *in vitro* Study with DNA fragmentation Assay. *Journal of Clinical & Experimental Pathology*, 2(2), pp. 1-5.

Nga, A.K.S., Tho, L.Y., Lim, C.H., Lim, C.K. and Say, Y.H., 2016. Evaluation of neuroprotective properties of two synthetic prenylated xanthone analogues against paraquat and 6-hydroxydopamine toxicity in human neuroblastoma SH-SY5Y cells. *Tropical Journal of Pharmaceutical Research*, 15(12), pp. 2611–2618.

Nimse, S.B. and Pal, D., 2015. Free radicals, natural antioxidants, and their reaction mechanisms. [photograph] *Royal Society of Chemistry Advances*, 5(35), pp. 27986–28006.

Niu, N. and Wang, L., 2015. *In vitro* human cell line models to predict clinical response to anticancer drugs. *Pharmacogenomics*, 16(3), pp. 273–285.

Olatunji, O.J., Chen, H. and Zhou, Y., 2016. *Lycium chinensis* Mill attenuates glutamate induced oxidative toxicity in PC12 cells by increasing antioxidant defense enzymes and down regulating ROS and Ca²⁺ generation. *Neuroscience Letters*, 616, pp. 111–118.

Pattalung, P., Wiriyaচিত্রা, P. and Ongsakul, M., 1987. The antimicrobial activities of Rubraxanthone isolated from *Garcinia parvifolia*. *Science Asia*, 14(1988), pp. 67- 70.

Pérez-Hernández, J., Zaldívar-Machorro, V. J., Villanueva-Porras, D., Vega-Ávila, E., Chavarría, A., 2016. A potential alternative against neurodegenerative diseases: Phytodrugs. *Oxidative Medicine and Cellular Longevity*, 2016(2016) pp. 1-19.

Qin, S., 2006. System Xc- and apolipoprotein E expressed by microglia have opposite effects on the neurotoxicity of amyloid-beta peptide 1-40. *Journal of Neuroscience*, 26(12), pp. 3345–3356.

Riss, T.L., Moravec, R.A., Niles, A.L., Duellman, S., Benink, H. Worzella, T.J., and Minor, L., 2013. Cell viability assays. *Assay Guidance Manual*, 114(8), pp. 785–796.

Rocha, M.D., Viegas, F.P.D., Campos, H.C., Nicastro, P.C., Fossaluzza, P.C., Fraga, C.A.M., Barreiro, E.J. and Viegas, C., 2011. The role of natural products in the discovery of new drug candidates for the treatment of neurodegenerative disorders II: Alzheimer's disease. *CNS and neurological disorders drug targets*, 10(2), pp. 251–270.

Shagufta and Ahmad, I., 2016. Recent insight into the biological activities of synthetic xanthone derivatives. *European Journal of Medicinal Chemistry*, pp. 267–280.

Sigma-Aldrich, 2017. *L-Glutamic acid 99%*. [photograph]. Sigma-Aldrich

Stansley, B., Post, J. and Hensley, K. 2012 A comparative review of cell culture systems for the study of microglial biology in Alzheimer ' s disease. *Journal of Neuroinflammation*, 115 (9), pp. 1–8.

Supasuteekul, C., Nonhitipong, W., Tadtong, S., Likhitwitayawuid, K., Tengamnuay, P. and Sritularak, B., 2016. Antioxidant, DNA damage protective, neuroprotective, and α -glucosidase inhibitory activities of a flavonoid glycoside from leaves of *Garcinia gracilis*. *Brazilian Journal of Pharmacognosy*, 26(3), pp. 312–320.

Suttirak, W. and Manurakchinakorn, S., 2014. In vitro antioxidant properties of mangosteen peel extract. *Journal of Food Science and Technology*, pp. 3546–3558.

Taher, M., Attoumani, N., Susanti, D., Ichwan, S.J.A. and Ahmad, F., 2010. Antioxidant activity of leaves of *Calophyllum rubiginosum*. *American Journal of Applied Sciences*, 7(10), pp. 1305–1309.

Tang, W.P., Pan, M.H., Sang, S.H., Li, S.M. and Ho, C.T., 2013. Garcinol from *Garcinia indica*: Chemistry and health beneficial effects. *ACS Symposium Series*, 1129(1), pp. 133–145.

Taylor, D.L., Diemel, L.T. and Pocock, J.M., 2003. Activation of microglial group III metabotropic glutamate receptors protects neurons against microglial neurotoxicity. *Journal of Neuroscience*, 23(6), pp. 2150–2160.

Thong, N.M., Quang, D.T., Bui, N.H.T., Dao, D.Q. and Nam, P.C., 2015. Antioxidant properties of xanthenes extracted from the pericarp of *Garcinia mangostana* (Mangosteen): A theoretical study. *Chemical Physics Letters*, 625, pp. 30–35.

Traber, M.G. and Atkinson, J. 2007. Vitamin E, antioxidant and nothing more. *Free Radical Biology and Medicine*, 43(1), pp. 4–15.

Upadhyay, S. and Dixit, M., 2015. Role of polyphenols and other phytochemicals on molecular signaling. *Oxidative Medicine and Cellular Longevity*. 2015(2015), pp. 1-15.

Wahyuni, F.S., Israf Ali, D.A., Lajis, N.H. and Dachriyanus, D., 2016. Anti-inflammatory activity of isolated compounds from the stem bark of *Garcinia cowa* Roxb. *Pharmacognosy Journal*, 9(1), pp. 55–57.

Xu, W., Huang, M.Q., Li, H., Chen, X.W., Zhang, Y.Q., Liu, J., Xu, W., Chu, K.D. and Chen, L.D., 2015. Chemical profiling and quantification of Gua-Lou-Gui-Zhi decoction by high performance liquid chromatography/quadrupole-time-of-flight mass spectrometry and ultra-performance liquid chromatography/triple quadrupole mass spectrometry. *Journal of Chromatography B: Analytical Technologies in the Biomedical and Life Sciences*, 986–987, pp. 69–84.

Xu, J., Gan, S., Li, J., Wand, D.B., Chen, Y., Hu, X., Yang. and G.Z., 2017. *Garcinia xanthochymus* extract protects PC12 cells from H₂O₂-induced apoptosis through modulation of PI3K/AKT NRF2/HO-1 pathways. *Science Direct*, 15(11), pp. 825-833.

Xu, W.J., Li, R.J., Quasie, O., Yang, M.H., Kong, L.Y. and Luo, J., 2016. Polyprenylated tetraoxygenated xanthenes from the roots of *Hypericum monogynum* and their neuroprotective activities. *Journal of Natural Products*, 79(8), pp. 1971–1981.

Yang, H.Y. and Lee, T.H., 2015. Antioxidant enzymes as redox-based biomarkers: A brief review. *BMB Reports*, 48(8) pp. 200–208.

Yew, M.Y., Koh, R.Y., Chye, S.M., Othman, I. and Ng, K.Y., 2014. Edible bird's nest ameliorates oxidative stress-induced apoptosis in SH-SY5Y human neuroblastoma cells. *BMC Complementary and Alternative Medicine*, 14(1), p. 391.

Yoswathana, N. and Esthiagi, M.N.E., 2015. Optimization of subcritical ethanol extraction for xanthone from mangosteen pericarp. *International Journal of Chemical Engineering and Applications*, 6(2), pp. 115–119.

Zhang, T.Z., Song, Z.J., Hao, J., Qiu, S.X. and Xu, Z.F., 2010. Two new prenylated xanthenes and a new prenylated tetrahydroxanthone from the pericarp of *Garcinia mangostana*. *Fitoterapia*, 81(6), pp. 595–599.

Zhang, S., Zhang, Y.Q. Li, H., Xu, W., Chu, K.D., Chen, L.D. and Chen, X.W., 2015. Antioxidant and anti-excitotoxicity effect of Gualou Guizhi decoction on cerebral ischemia/reperfusion injury in rats. *Experiment and Therapeutic Medicine*, 9(6), pp. 2121-2126.

APPENDIX

APPENDIX A

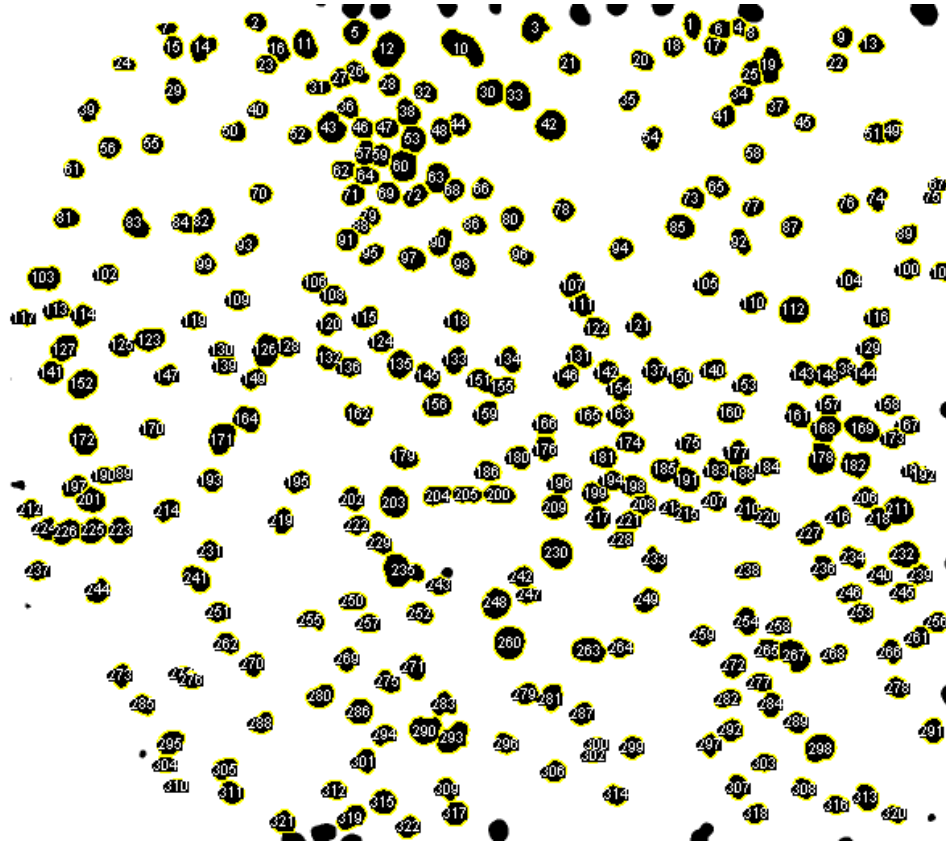


Figure 1: BV2 cells in growth control after thresholding and measurement. The label indicated the cells included in measurement of nuclear area and circularity.

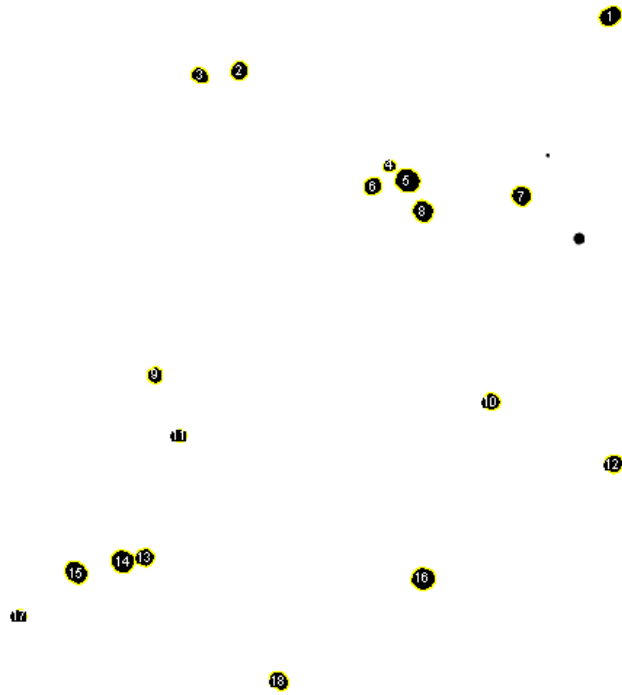


Figure 2: BV2 cells in co-treatment of vitamin E with glutamate after thresholding and measurement. The label indicated the cells included in measurement of nuclear area and circularity.

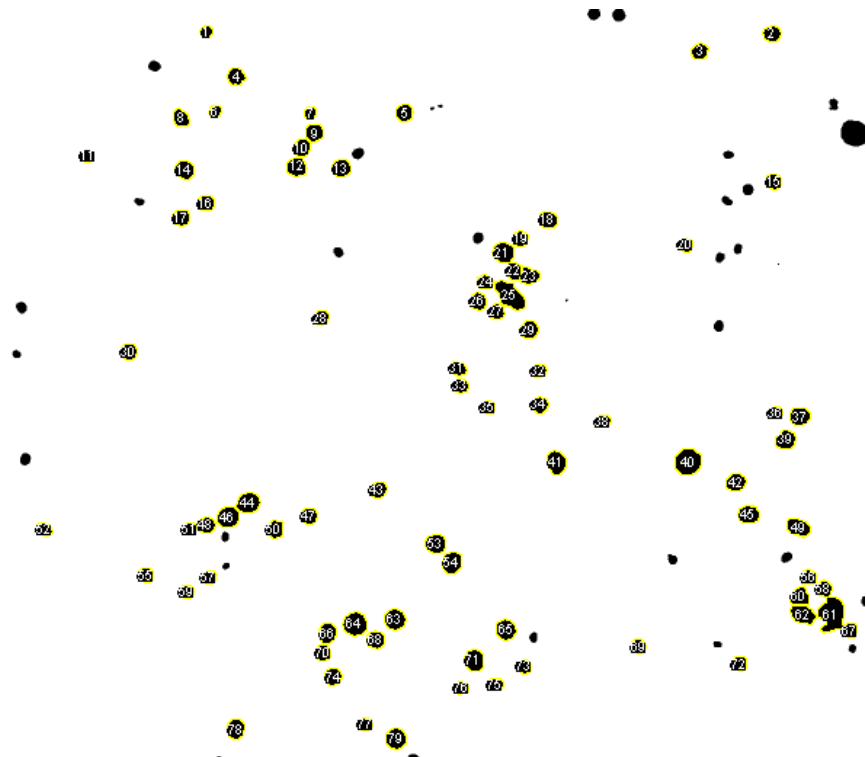


Figure 3: BV2 cells in glutamate treatment only, after thresholding and measurement. The label indicated the cells included in measurement of nuclear area and circularity.

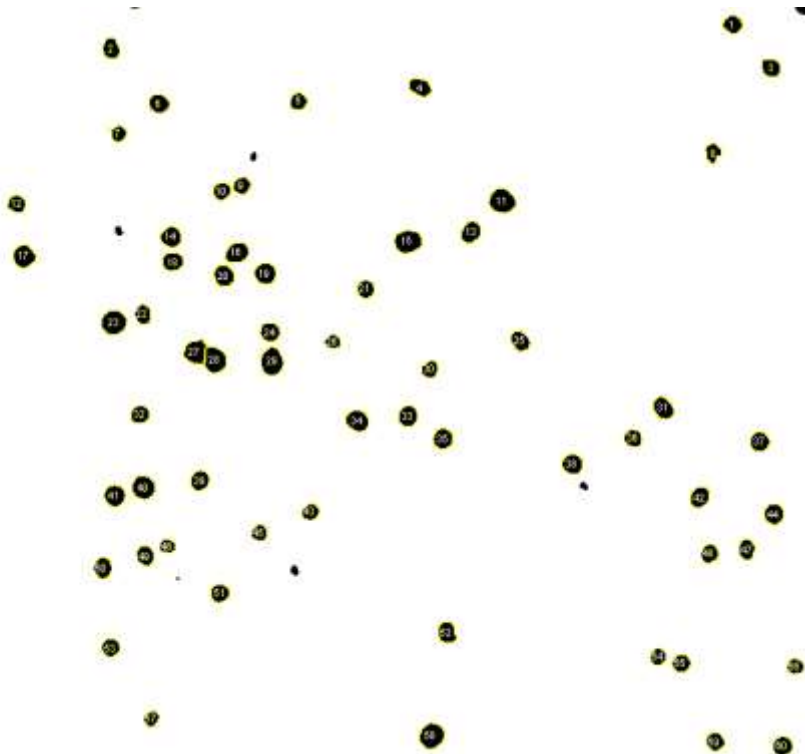


Figure 4: BV2 cells in co-treatment of EX with glutamate after thresholding and measurement. The label indicated the cells included in measurement of nuclear area and circularity.

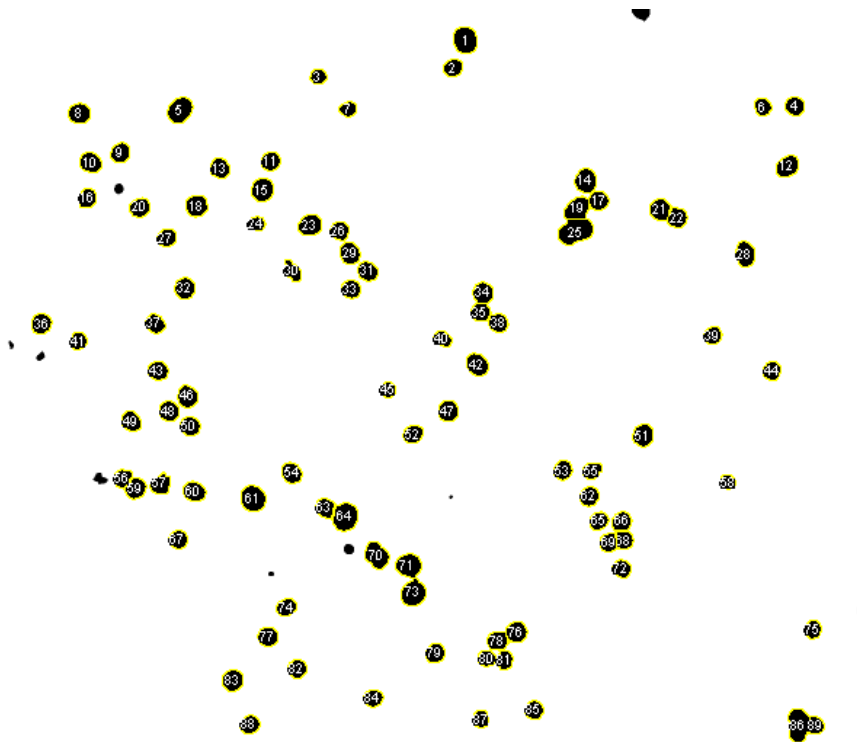


Figure 5: BV2 cells in co-treatment of AX with glutamate after thresholding and measurement. The label indicated the cells included in measurement of nuclear area and circularity.

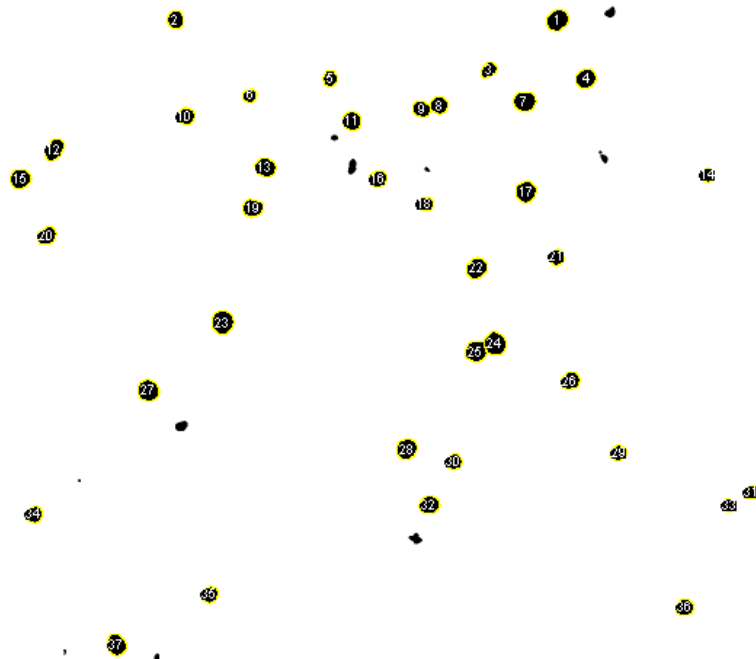


Figure 6: BV2 cells in co-treatment of RX with glutamate after thresholding and measurement. The label indicated the cells included in measurement of nuclear area and circularity.

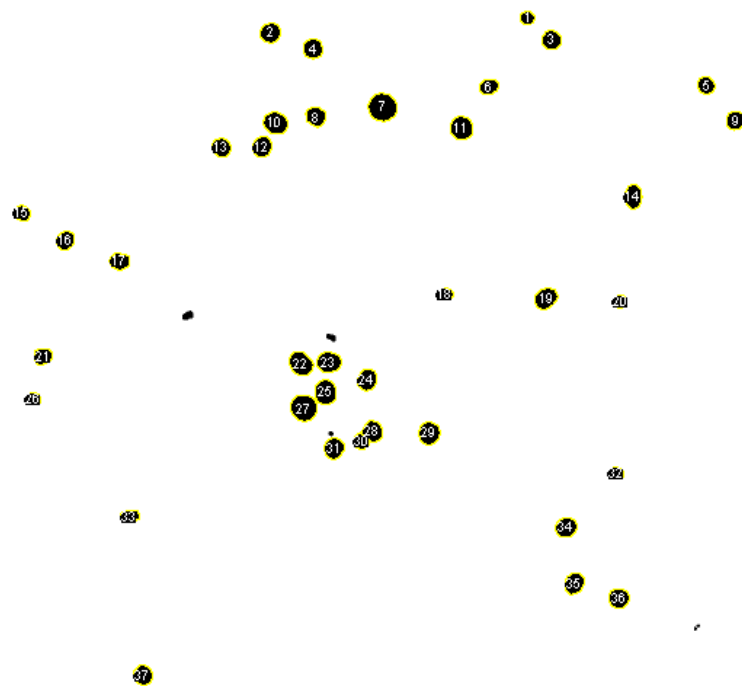


Figure 7: BV2 cells in co-treatment of TX with glutamate after thresholding and measurement. The label indicated the cells included in measurement of nuclear area and circularity.